Linköping University | Department of Management and Engineering
Master's thesis, 30 credits| Applied Mechanics
Spring 2025| LIU-IEI-TEK-A--25/05090--SE

Numerical Simulation of Lamb Wave Propagation for Detection of Damage in Composite Structures

Marcus Lundgren
Gustav Lindström

Supervisor: Joakim Holmberg
Examiner: Carl-Johan Thore

Industrial Supervisor: Ruoshan Luo

Linköping University
SE-581 83 Linköping, Sweden
+46 013 28 10 00, www.liu.se

Upphovsrätt

Copyright

Abstract

With the increasing use of composite materials in the aerospace sector, ensuring their structural integrity is critical. As the industry progresses toward sustainability in material usage, Structural Health Monitoring (SHM) is emerging as a key approach for evaluating structural integrity without causing damage. By continuously monitoring the structural health, the material's lifecycle can be extended, reducing material waste and supporting more efficient use of resources.

This study investigates numerical simulation of Lamb wave propagation using the finite element program LS-DYNA, with the aim of developing a methodology for damage detection in composite structures. The robustness of the methodology is evaluated by analyzing a composite plate under various damage modes and composite material models using different Lamb wave signals. To model the composite plate, thin layers were assigned shells element formulations and stacked to resemble a composite structure. Lamb wave propagation was simulated with the excitation signal defined as a prescribed displacement instead of modelling the sensors used in SHM systems.

With a final composite plate model, cracks and delaminations were introduced into the plate, where simulations compared the results from intact and damage plates. The method relies on exciting the Lamb wave signal at a selected excitor node, from which the wave propagates through the plate and the signal data is collected at a receiver node. If a damage is present, the readings at the receiver node will differ from that of an intact plate.

The simulations showed that damage such as cracks and delaminations can successfully be detected and localized. The study shows that both amplitude reduction and temporal delay of the wave signal indicates the presence of a damage. The wave interaction with damage suggests potential for characterization of damage modes. Testing various frequencies for the excitation signal demonstrates that higher frequencies are more effective for smaller damages, while lower frequencies are suitable for detecting larger damages. This highlights the importance of selecting frequency based on the criteria for what types and sizes of damage are considered critical for structural integrity.

Acknowledgements

We would like to extend our deepest gratitude to Saab for the exciting opportunity to prove our engineering knowledge and for their guidance throughout our thesis.

We are especially grateful to our industrial supervisor Ruoshan Luo for her continuous encouragement and feedback throughout the entire work, guiding us towards the mutual goal, and Daniel Lindbom for his support and insights.

From Linköping University, we would like to thank our supervisor Joakim Holmberg for his guidance in improving the quality of the thesis and Carl-Johan Thore for assuring the academical reach while also providing insightful feedback.

Finally, we would like to thank David Aspenberg for his technical support regarding LS-DYNA.

Linköping, June 2025
Gustav Lindström & Marcus Lundgren

Contents

List of Figures:

List of Tables:

1 Introduction

1.1 Background

With the current push towards the use of composite materials in the aerospace sector, due to its high strength-to-weight ratio, the need to maintain and control the structural integrity of the parts increases. Structural Health Monitoring (SHM) integrates a sensor monitored structure with a system of algorithms that continuously evaluates the structural condition in real time. Using an SHM system can improve safety and reliability while reducing downtime and maintenance cost. SHM is regularly used in mechanical and aerospace engineering structures, where the primary goal is to locate damage as well as structural failure in the early stages before the damage leads to catastrophic failure that can compromise safety [1].

To avoid catastrophic failures for an aircraft, the composite material has a set lifespan based on experimental data. The composite material is often decommissioned before its actual life cycle has been completed, resulting in unnecessary material costs and environmental impacts. Traditional techniques often involve dismantling the composite to investigate its structural health, which can be avoided using SHM. By investigating the use of SHM and Lamb waves to detect whether the structure is damaged before disposing of it, significant cost savings and reduced environmental impact can be achieved.

A common approach in SHM is to use low-frequency methods for damage detection [2]. However, a limitation of this approach is that it is often unable to detect small damages, such as delamination or fiber cracks frequently found in composites. A remedy for this limitation is the use of Lamb waves, named after the mathematician Horace Lamb, that are being generated and sensed with surface bonded piezoelectric (PZT) transducers for detection of small damages in a SHM system. Lamb waves are guided elastic waves that can travel long distances within thin structures, and their interaction with defects such as cracks or delaminations cause noticeable changes in wave propagation, enabling damage detection [3]. An illustration of a typical setup for Lamb wave propagation is shown in Figure 1.1.

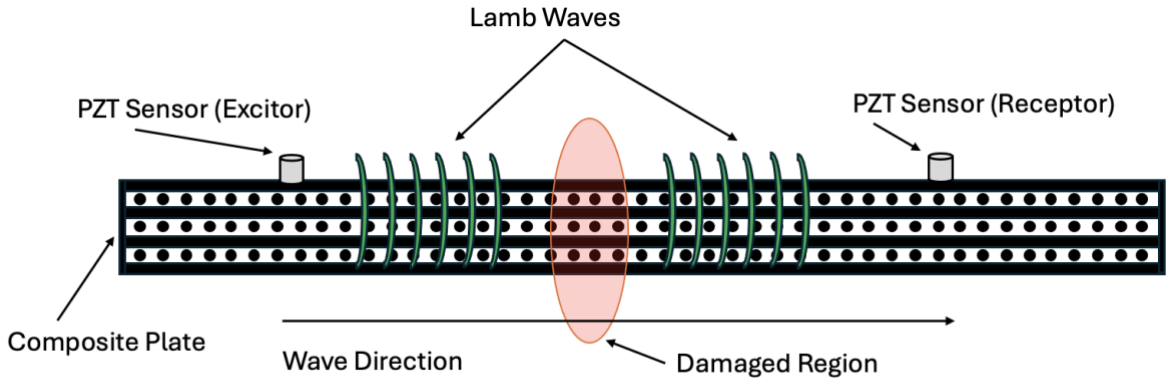

Figure 1.1: PZT transducers applied to the top of the composite plate, where one of the transducers acts as an excitor that generates Lamb waves. The Lamb waves propagate through the composite plate and are then sensed in the PZT transducer acting as a receptor.

The use of numerical simulation of Lamb wave propagation has the potential to become a powerful tool for detection and prediction of damage in composite structures.

Nevertheless, there are known challenges in terms of modelling accuracy, sensitivity to boundary conditions, and complexity when simulating small-scale damage.

1.2 Problem Description

The main purpose of this study is to investigate how numerical simulation of Lamb wave propagation can be used to detect damage in a composite material. The objective is thus to develop a predictive modelling methodology using a finite element program. This will be conducted at Saab, where the methodology is to be applicable for damage detection in a composite material used for an aircraft radar structure.

The numerical simulations in this work will be conducted using the finite element program LS-DYNA, which enables an explicit simulation of Lamb waves and the modelling of complex material behavior of composites. By simulating different damage and wave signals, the study aims to investigate what types of composite damages can be detected and determine whether the method is reliable. Additionally, the analysis will examine whether Lamb wave propagation can be used to localize and characterize the defect.

1.3 Research Questions

The following research questions shall be answered in this study:

R.1: How can numerical simulations of Lamb wave propagation be applied to detect damages in composite materials?

R.2: How reliable is the Lamb wave damage detection method in detecting different damages in composite materials?

1.4 Project Planning

The approach for the study is divided into several stages:

1. Literature review
2. Theoretical framework based on previous research
3. Project Methodology
4. Results, discussion, and conclusions

A methodology is developed, based on the theoretical framework, to implement existing techniques to fit the desired application. The results are then interpreted to answer the research questions and provide a conclusion.

1.5 Delimitations

To ensure that the study remains within a reasonable timeframe and scope, the following delimitations are made:

The purpose of the study is to develop a methodology that provides reliable response when detecting defects in a composite material. The method shall be applicable for damage detection in a real-world application, but this study will be limited to examining

a simplified geometry starting with a rectangular plate. Defects modelled in the plate are mainly small-sized matrix cracks and delamination in the composite material. Thus, the study does not focus on other types of defects.

The study will not consider any specific environmental or thermal effects that may affect the mechanical properties of the composite material. The study is conducted in such manner to replicate an experimental testing environment, where the contribution of such factors is limited to increase the validity of the experiment.

Experimental testing of the Lamb wave application will not be investigated in this study, as the main purpose is to develop a methodology for numerical simulations. The sensor system used when monitoring the wave propagation in experimental testing is thus not relevant as this is only done by simulation. Hence, only a brief explanation of the sensor function in this application is given.

1.5.1 Later Delimitations

The initial scope included the investigation of modelling actual surface bonded piezoelectric transducers assigned an excitation signal. However, difficulties in obtaining material data for the transducers led to the later delimitation of only defining the excitation signal as a nodal displacement.

1.6 Literature Review

Under the topic of damage detection using guided waves in a material, a variety of related research can be found. Some are delimited to the exploration of a single frequency wave to determine the accuracy of the simulation model in detecting damage, while other research focuses on the efficiency of the wave itself, testing different types, modes and frequencies.

Relevant research primarily focuses on guided waves for damage detection and the modeling of composite materials. There are several approaches to modeling the stacking of layers for composite materials and previous research has evaluated some of the most basic ones. Depending on what features are required for the application, the composite material model can be most simply defined by either creating a stack of individual parts as layers (stacked layer method) or by using one single layer of elements and defining the composite layers within this part, which will be presented in Chapter 3. Both approaches correctly define the composite material model, but they come with different limitations and advantages. The approach that requires the least computational effort is the single layer element method, but this model is limited in the ways damage modes can be defined. The stacked layer method has a lot of freedom when modeling the damage, but at a high computational cost as the model has a significantly higher number of elements [4].

To ensure that the mesh does not interfere with the Lamb wave signal, the maximum element size is determined from the wave signal. According to [5], an effective approach is to have at least 10-20 elements per wavelength. However, even when selecting an element size based on this criterion, the mesh may still require further refinement for the specific application.

Moreover, previous studies have also investigated potential simplifications in the numerical simulations of damage modes. The simplifications in these studies have primarily focused on using degraded material properties in the damaged region in the composite, instead of modelling the actual damage. Such simplifications can be made to reduce time and labor costs, since modelling accurate damage modes often is a difficult and complex process [6]. Meanwhile, degradation of material properties in the model requires reduced material data which must be obtained either from experimental testing or knowledge in composite degradation.

Several previous studies have compared numerical testing using FE models with physical experiments. The experiments will not be reviewed in detail, as this study does not conduct any experiments to validate results. However, previous experimental research has shown that the FE simulations and physical experiments have a good agreement, which supports the reliability of the numerical results [7].

Further research should include analyzing the relative positions between sensors and comparing different severities of delamination damage [8]. This study investigates the method for a single static damage case, which is useful for verifying its accuracy. However, it does not account for how the numerical model responds to damages of varying severities or other damage modes. Additionally, the study tests the method with only one sensor placement, which could compromise the validity of the results if the method was applied to a different placement, as the wave travel distance is crucial for the wave characteristics.

While multiple studies have shown that Lamb waves can detect damage in structures, they do not focus on locating the damage [6]. Getting information about the position of the damage simplifies maintenance and helps identify weaknesses in the structure, making the localization of the damage an important aspect of this study.

Related research includes the use of Lamb waves for damage detection in composites, but also for other materials such as metals [9]. The software used for simulation differs between previous research but is mainly performed using an explicit solver.

1.7 Outline

The remaining chapters of this study are briefly explained below:

Chapter 2: Theoretical Framework
- Key theoretical concepts, principles and terminology that are essential for understanding the method, results and discussion in the following chapters.

Chapter 3: Method
- The methodology used for the implementations in LS-DYNA. It builds on the theoretical framework and provides a detailed explanation of the key steps taken to obtain the results.

Chapter 4: Results & Discussion
- Results from the implementations based on the methodology and discussion of the results, methodology, improvements, and future work.

Chapter 5: Summary
- Summary of the study, answers on the research questions, and future areas of improvement.

2 Theoretical Framework

2.1 Composites

The use of composites in the aerospace sector is increasing rapidly, primarily due to their high strength-to-weight ratio, stiffness, and ability to tailor their properties for specific applications.

A composite consists of at least two constituent materials, e.g. a polymer matrix that has been reinforced with fibers. This combination of two materials allows the fibers to carry load along the fiber direction while the matrix disperses stress among the fibers and acts as a bond to keep the fibers in place [10]. A variety of fiber types exist, with common types being carbon, glass, or flax.

Composite materials are typically constructed by stacking plies, i.e. several layers that are bonded together. The orientation of the fibers in each ply and the layering order will provide the composite with different mechanical properties in certain directions. To better understand the properties of a composite material, the different fiber orientations can be classified in three categories: unidirectional (UD), where all fibers are aligned in the same direction; bidirectional where the fibers are arranged in two perpendicular directions; and multidirectional which has fibers arranged in multiple directions.

By assessing the use of the composite material, the optimal layup can be designed. What this means is that if the application requires the composite material to be stronger in a specific direction, the plies are typically stacked with more fibers oriented in that direction [11]. For further details on this topic, see [12].

2.1.1 Damage Modes

The complicated nature of composite laminates makes it complex to predict their failure modes. In contrast to traditional materials such as metals, composite laminates may fail in several different modes that interact and influence each other [13]. In this work, interlaminar delamination and matrix cracks will be investigated.

Interlaminar delamination refers to the separation of two plies in a composite material, shown in Figure 2.1. This occurs when the plies have insufficient bonding between them or when the composite is exposed to excessive stress. Interlaminar delamination is a significant failure mode that weakens structural integrity and reduces mechanical strength. It can result from mechanical stresses like impact or fatigue as well as defects that occur during manufacturing such as poor bonding or voids between the plies. Delamination can lead to progressive failure, which is critical in aerospace applications where durability is essential [14].

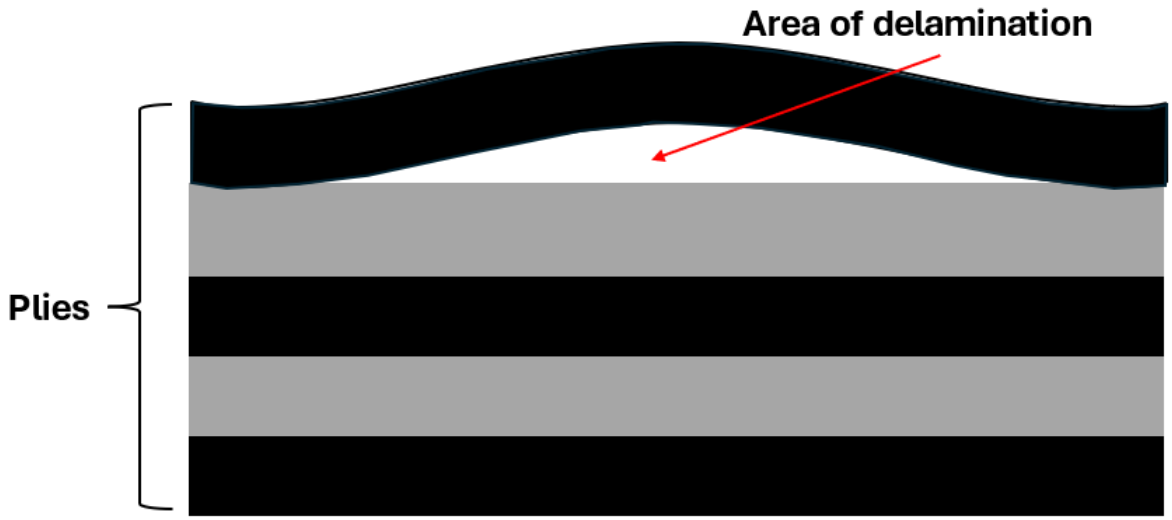

Figure 2.1: Interlaminar delamination between two plies.

Matrix cracks usually occur perpendicular to the fiber direction and are commonly referred to as transverse cracks. Unlike visible surface cracks, transverse cracks propagate through the thickness of a ply, as shown in Figure 2.2.

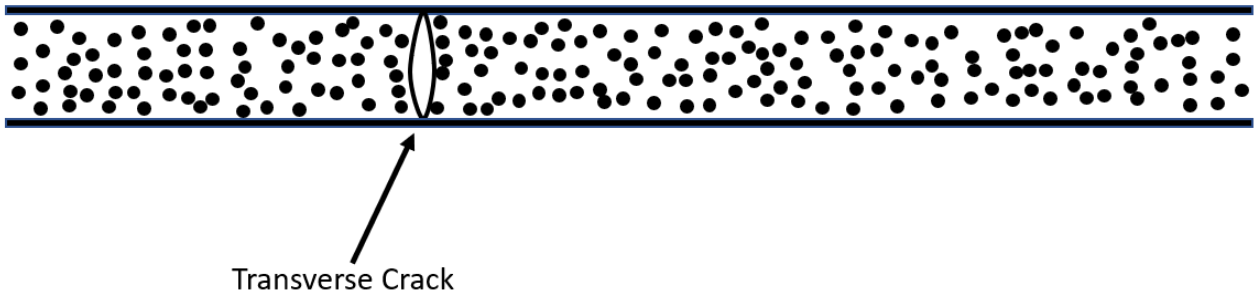

Figure 2.2: Transverse crack through the thickness of a composite ply.

These cracks are often caused by tensile, shear or thermal stress. They typically develop during processing or under mechanical loading during use in the application. While matrix cracks do not directly affect the fiber strength, they weaken the overall structure and can lead to further damage such as delamination or fiber breakage. If left undetected, matrix cracks can propagate and significantly impact the performance and durability of the composite structure. Therefore, it is important to detect this type of damage in an early stage to prevent further degradation and reduce the risk of failure [15].

2.2 Structural Health Monitoring

Structural Health Monitoring (SHM) is a system that utilizes Non-Destructive Testing (NDT) methods with the ability to detect and interpret damages and defects in a structure, aiming to improve reliability and reduce life-cycle costs. The SHM system is automated and involves using sensors and data analysis techniques to continuously

monitor a structure's condition and identify any defects. When defining the SHM architecture, damage characteristics of the structure plays a significant role. This determines the selection of sensors and the requirements for other components within the structure. The sensors are used to measure changes in the structure's natural frequencies, where these changes can indicate damage [16].

Barely Visible Impact Damage (BVID) is a prime example of the type of damage SHM is designed to detect. BVID is damage that usually cannot be detected by human observation. Defects such as delamination and matrix cracking within the composite material, or microcracks on the surface are types of BVID. These are initially minor defects that weaken the structure over time and could possibly result in failure [17].

Other types of non-automated NDT techniques include ultrasonic testing inspection through the methods Pulse-echo, Through-transmission, and Pitch-catch, as well as radiographic testing [18]. The three ultrasonic testing methods all have a simple setup and can be used for various materials but lack the extensive area coverage and suitability for composite materials that Lamb wave propagation offers.

Lamb waves are used for continuous monitoring of structures, which makes them a suitable choice for SHM systems. Their ability to not only detect the presence of a defect but also the severity and type of damage exceeds the capabilities of traditional frequency response methods. The sensitivity of Lamb wave techniques to anisotropy in a composite material enables them to effectively detect various types of damage such as delamination and transverse cracks [19]. However, Lamb wave modes are challenging to analyze due to them being naturally dispersive [20], meaning that the wave speed depends on the frequency.

This study will simulate the use of PZT sensors to generate Lamb waves of specific frequencies within a structure. By analyzing changes in these wave frequencies over a structure, the use of Lamb waves can detect potential defects.

2.3 Lamb Wave Propagation

Lamb waves are a type of elastic wave that propagates in thin-walled structures such as thin plates or shells. Lamb waves are guided along surfaces, and their behavior depends on the geometry and thickness of the structure. Variations in frequency and structure thickness affects the wave speed and this determines the sensitivity to structural features and defects.

Lamb waves have a high sensitivity to damage, making them ideal for detecting defects. When the waves encounter a defect in the thin structure, they exhibit mode conversion, scattering, reflection and transmission, which help locate the damage. Scattering occurs when a Lamb wave hits a defect, causing the waves to change direction and spread out. The Lamb waves can also directly reflect when reaching a boundary such as a defect and the wave bounces back in the opposite direction. These effects on the wave will result in a change in amplitude or a time delay, which is analyzed to detect a defect. Lamb waves can also help characterize the type of damage as different frequencies and modes are sensitive to certain defects [21].

The effectiveness of Lamb waves revolves around its capability of travelling a long distance even in materials with a high attenuation ratio, which is practical when examining composite materials. Additionally, the propagating characteristics of the waves depend on only two material properties for an isotropic case, namely the stiffness E and the density ρ of the material. That is, the wave speed v is determined from:

$$v = \sqrt{\frac{E}{\rho}}$$

The wave speed should thus decrease for a less stiff material, which is a relevant feat to consider in terms of material degradation of damage impacting the material stiffness. Lamb waves can cover large areas and are capable of detecting small defects, making Lamb waves a favorable method for non-destructive damage detection applications. Additionally, when it comes to material anisotropy, Lamb waves applications are more robust in real-world conditions [13].

2.3.1 Wave Modes

Lamb waves have two primary modes: symmetric (S-modes) and anti-symmetric (A-modes). S-mode waves move along the surface of the structure, while the A-mode waves travel through its thickness, shown in Figure 2.3. The zero order modes, S_0 and A_0, i.e., the modes with the lowest frequency have gained attention due to its capable damage detection characteristics. More specifically, the A_0-mode has received interest because of its shorter wavelength, slower phase velocity, and higher spatial resolution compared to the S_0-mode, making it an appropriate fit for damage detection [22]. This means that the A_0-mode is highly sensitive to variations in the material properties through the thickness, which is advantageous since the wave will be strongly reflected from voids such as delaminations or cracks. This study will only investigate the use of A_0 for damage detection, as the damage to be detected will be modelled inside the composite.

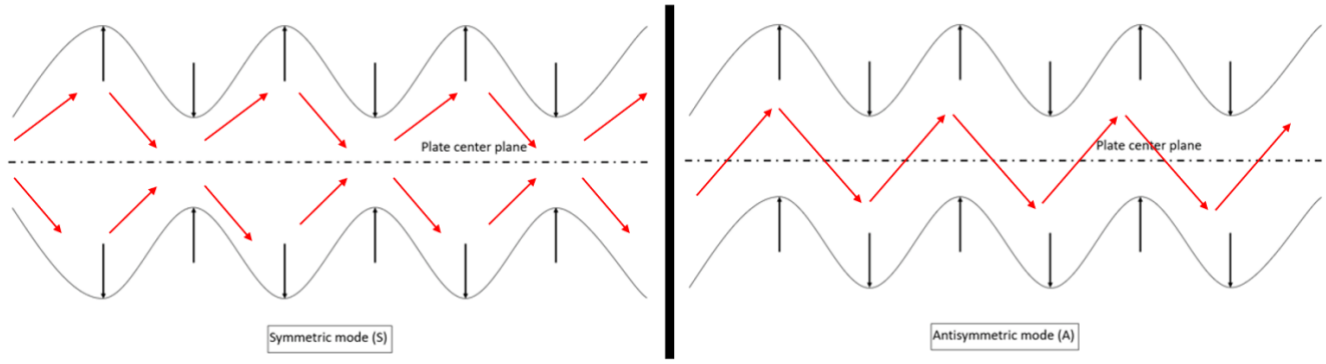

Figure 2.3: Lamb wave behavior of (a) Symmetric mode; (b) Antisymmetric mode.

2.3.2 PZT Sensors

A piezoelectric lead zirconate titanate (PZT) sensor is a common approach to send and detect Lamb waves. PZT sensors are commonly connected to electric wires and glued to the surface of the structure and utilize the charge created when mechanical stress is applied to measure voltage through the material [23]. When used for damage detection, the sensor is excited by the charge which then vibrates the material by converting the

charge into ultrasound waves. The waves travel through the material and are reflected or scattered by internal structures, damages like cracks or delaminations, and surface irregularities. It should be noted that the vibrations from the sensors are insignificant to the structural health of the material and will not cause any damage. The acquisition of the signals is done through PZT sensors acting as receptors placed on the material, which enables storage of the signals through receiver boards connected to the PZT receptors [19]. An illustration of the setup is shown in Figure 2.4.

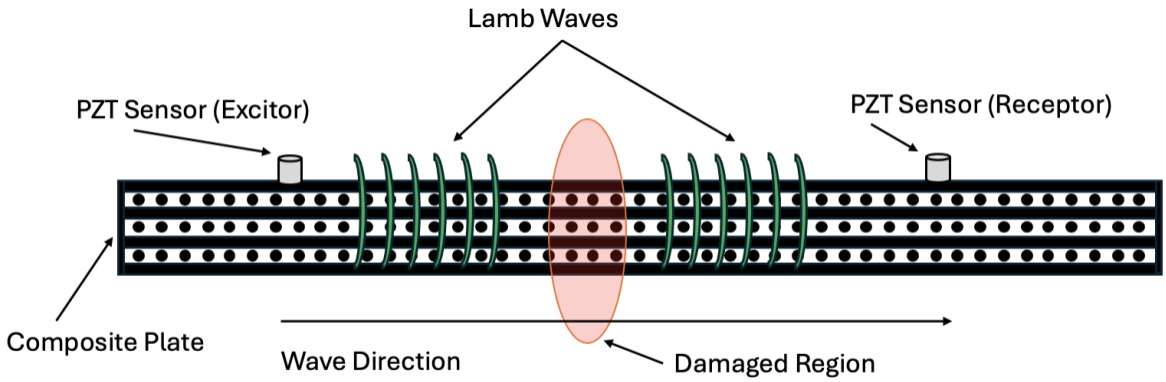

Figure 2.4: PZT sensors applied to the composite plate, with the Lamb waves propagating over the damaged region.

2.3.3 Hanning Window

When evaluating the use of Lamb waves for damage detection, a suiting excitation signal needs to be obtained. Typically, a windowing function is multiplied with the excitation signal function to reduce spectral leakage and improve frequency resolution. This is particularly important when using signals with low bandwidth like a short-duration signal consisting of a few cycles of a sinusoidal waveform, which are commonly used to excite specific Lamb wave modes [24].

Since Lamb waves are dispersive, with different frequencies traveling at different velocities, controlling the frequency content is crucial for accurately isolating wave modes. This allows for better separation between symmetric and anti-symmetric modes, which can overlap in complex structures. Windowing improves wave propagation analysis and enhances the accuracy of damage detection [25].

The Hanning window function is the most used due to its effectiveness in enhancing frequency clarity. It smooths the signal at its endpoints, preventing unwanted frequency components. By smoothing the signal edges, the Hanning window minimizes time-domain discontinuities and eliminates abrupt start and end transitions.

The standard Hanning window function is given by:

$$w(n) = 0.5\left(1 - \cos\left(\frac{2\pi n}{N-1}\right)\right)$$

where $w(n)$ is the value of the window function at sample index n, which ranges from $0\ to\ N-1$ and N is the total number of samples i.e. the length of the window.

Multiplying by 0.5 scales the peak value to 1 and ensures smooth, bell-shaped curve. An example for a total number of samples of 1000 is shown in Figure 2.5.

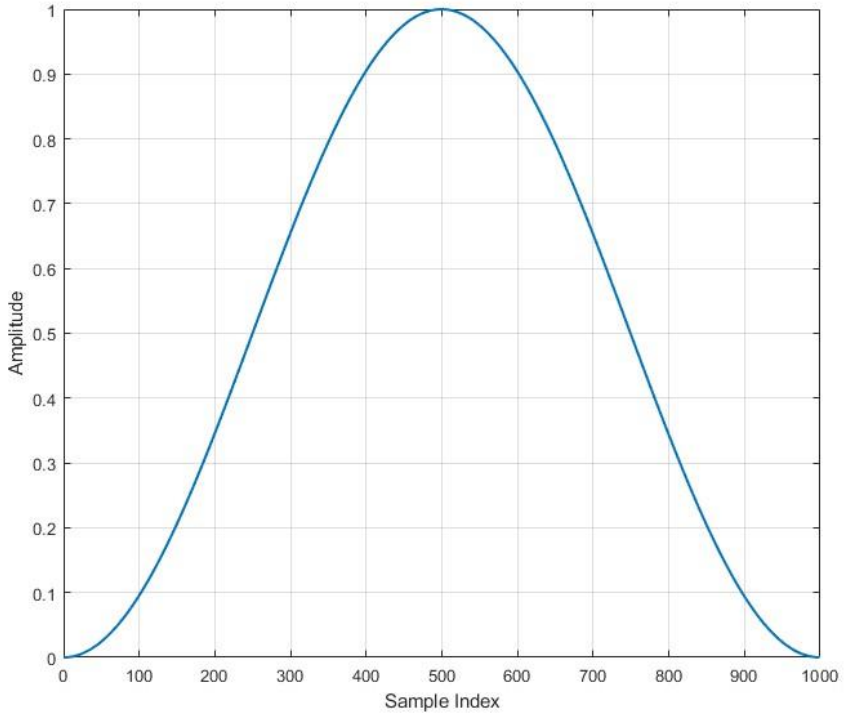

Figure 2.5: Hanning window function for 1000 samples.

2.3.4 Dispersion Curve

That Lamb waves are dispersive means that their phase velocity depends on the frequency. Different wave modes propagate at different speeds and using the correct wave function is crucial as it influences the wave's sensitivity to damage. The dispersion curve shows how the phase velocities vary with frequency for the different wave modes. The exact behavior depends on material properties and the structure's thickness. Analyzing the dispersion curves for the specific structural thickness and material helps in selecting appropriate frequencies. Furthermore, dispersion curves can be used to see the inspection distance that can be covered, as the propagation distance can be obtained [26]. The specific dispersion curve used in this study will be presented Chapter 3.

2.4 Modelling Criteria

2.4.1 Mesh Criteria

Models used for wave propagation simulations must follow general meshing criteria to ensure accurate capture of wave characteristics. The element size should be small enough to resolve the wavelength λ, and a common approach is thus to have at least 10 elements per wavelength [5].

The wavelength (λ), is defined using the Lamb wave phase velocity (c_p) divided by its frequency (f) as:

$$\lambda = \frac{c_p(f)}{f}$$

The element size, Δx, represents the length of a mesh element (i.e. the maximum distance between adjacent nodes in the mesh). With the criteria of at least 10 elements per wavelength this gives the criteria for the maximum element size Δx:

$$\Delta x \leq \frac{\lambda}{10}$$

This criterion must be fulfilled to ensure numerical stability.

2.4.2 Timestep Criteria

In wave analysis, selecting an appropriate timestep is crucial for capturing the wave propagation. The timestep must be small enough to resolve the wave motion without causing instability. One common way for ensuring numerical stability in explicit time integration schemes is the Courant-Fredrichs-Lewy (CFL) criterion. This criterion ensures that the timestep Δt is small enough so that the numerical solution stays in sync with the actual wave behavior. This is expressed mathematically as:

$$C = \frac{c_p \Delta t}{\Delta x} \leq C_{max}$$

In this formula, C_{max} is the critical value of the Courant number (C) that ensures numerical stability and is typically within the range of 0.5 to 1 for explicit methods. The Courant number, C_{max}, can be considered as a safety factor, usually obtained by empirical testing. The phase velocity governs how fast the wave propagates through the material. By rewriting this equation, the critical timestep is obtained:

$$\Delta t \leq \frac{\Delta x}{c_p} C_{max}$$

If the timestep is too large, the simulation might experience nonphysical oscillations or divergence. However, selecting an excessively small timestep significantly increases the computational cost, highlighting the importance of choosing a timestep based on the CFL criterion [27].

3 Project Methodology

The numerical simulations are conducted using LS-DYNA, which is a simulation software that uses the Finite Element Method (FEM) to model dynamic events implicitly or explicitly [28]. All results are investigated using LS-PrePost(R) version 2024/R2(4.11.3) and LS-Run 2024 R2.

3.1 LS-DYNA Keywords

To define the simulation setup in LS-DYNA, a modelled mesh and a set of keywords to control the simulation are required. Keywords are predefined software commands that are used for the setup of the model. In the keywords, material properties, boundary conditions such as loads or contacts, and timesteps can be defined which are then used to control the simulation. A keyword starts with an asterisk (*) and is followed by a word to define what the user wants to control, e.g. the material, boundary conditions or prescribed motions, and more commands. As an example, *MAT_058-LAMINATED_COMPOSITE_FABRIC is used to alter the material properties of a composite material, where MAT_058 states the material number 58 followed by the name of the material. All keywords used for the model definition in this study are presented in Appendix A. The FEM simulations conducted are linear, as small deformations and linear elasticity are assumed and solved explicitly. To minimize the risk of numerical errors, all element formulations investigated are fully integrated for maximum accuracy, and the timesteps and mesh size used are selected to ensure stable wave propagation. Furthermore, other time integration methods such as mass scaling is not considered in this study as this can influence the accuracy of the results if it is not used correctly. All other parameters used in the simulations are run with default settings for LS-PrePost version 4.11.3.

3.2 Modelling of Composite Plate

The numerical modelling of a composite plate is used to create a digital twin, i.e. a dynamic simulation that reflects the behavior of a real-world physical version. The composite is modelled as a square plate with a length and width of 0.1 m and consists of 32 plies with an individual thickness of 0.125 mm per ply, resulting in a total thickness of 4 mm. Such simple geometry is used since this study does not intend to simulate a specific problem or geometry but rather focuses on developing a general methodology to be implemented in future work. In LS-DYNA, the mesh is created by selecting an element type and defining the number and distribution of elements desired to cover the geometry of the model.

The composite used for the simulations is CFRP T700S with a layup of $[0\ 90\ 45\ -45]_{s8}$, where *s* means that the layup is symmetric, i.e. the stacking sequence is mirrored about the mid-plane of the laminate, and *8* means that the sequence is repeated 8 times resulting in 32 plies in total. The plies have UD fibers, meaning that the fibers are all oriented in the same direction within each ply, enabling the layup to govern the material properties in different orientations.

When modelling a composite in FE software, the layer stacking poses a challenge in terms of computational time, as each layer could require its own set of elements. There are several methods to model elements in LS-DYNA, shown in Figure 3.1, each influencing the modelling and simulation time. Method A focuses on creating a composite part using the keyword *PART_COMPOSITE, where plies can be stacked, oriented, and given thickness within a single shell based on one integration point through the thickness. Although this results in a significantly lower number of elements for the composite part, this approach limits the modelling of damage modes as delamination between two plies cannot be modelled within a single layer. Thus, using this method on its own is not suitable for the application in this study as detection of small damages is investigated.

Method B uses a solid element formulation, modeling each layer with its own set of elements, which allows greater flexibility in simulating various damage modes. However, this method requires significant computational effort, leading to long simulation times.

For thin structures, shell elements are generally preferred, as they require less computational effort. Due to the thin nature of the composite to be modelled, a suitable option could be to use method C which decreases the computational time by instead stacking thin shells layers to form the composite part. Although this is an efficient element formulation, modelling many layers representing each ply in the composite individually could result in a slow model even with a coarse mesh. The last approach is therefore to use method D, which is a hybrid of element formulations, using both shell and solid elements. Method D can be applied to any number of stacked shell elements, modelling additional solid element layers between each set of shell layers. In this formulation the solid elements are defined as cohesive elements, which act as the contact interface between the shell layers. The cohesive solid elements connect all the plies, enabling them to function as a unified structure.

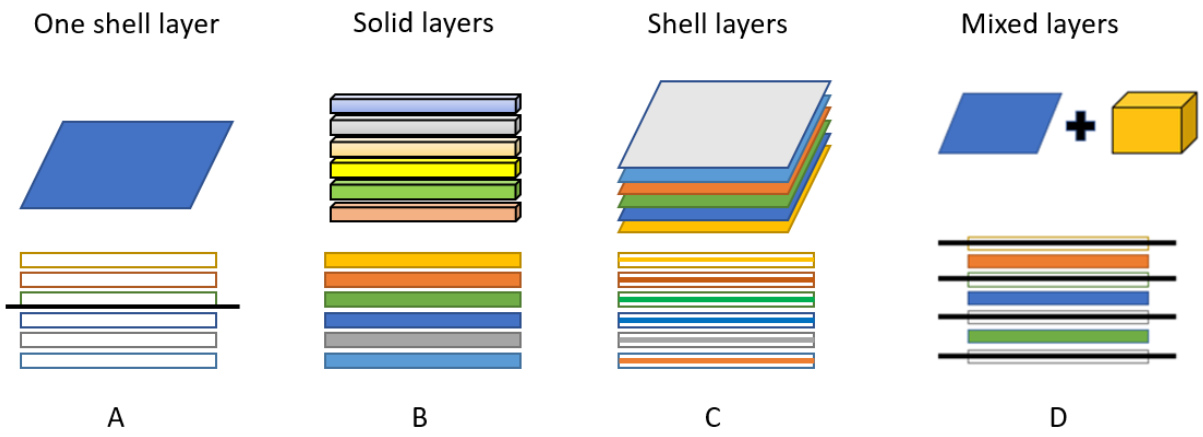

Figure 3.1: The different element formulation methods, with the black lines corresponding to the integration points of the one shell layers.

3.2.1 Choice of Element Formulation

Due to its potential of minimizing the simulation time, method D is investigated. This is performed by combining shell elements with the keyword *PART_COMPOSITE and solid cohesive layers between the shell elements. Four thin shell plates are modelled as 0.1x0.1 m squares, where each shell plate is assigned a thickness of 1 mm. The shell plates

are defined as composites with the *PART_COMPOSITE keyword, each assigned an 8-ply layup given as $[0\ 90\ 45\ -45]_s$, resulting in 32 plies in total.
The plies are assigned to the thickness 0.125 mm and material properties are defined in a separate material keyword. The material properties are presented in Table 3.1. The cohesive layers placed between the shell plates are given a small thickness to not disturb the simulations, i.e. they are only modelled to act as a bond between the layers.

The cohesive elements are beneficial for simulating delamination. However, since the modeled delamination is static and there will not be any external forces that could create further delamination, the use of cohesive elements might be excessive.

Table 3.1: Composite properties defined in the material keyword.

ρ [kg/m^3]	1800	Material density
E_1 [GPa]	139	Young's modulus in the fiber direction
E_2 [GPa]	8.5	Young's modulus in the transverse 2-direction
E_3 [GPa]	8.5	Young's modulus in the transverse 3-direction
G_{12} [GPa]	4.2	Shear modulus in the 12-direction
G_{13} [GPa]	4.2	Shear modulus in the 13-direction
G_{23} [GPa]	2.2	Shear modulus in the 23-direction
ν_{12} [-]	0.24	Poisson's ratio in the 12-direction
ν_{13} [-]	0.24	Poisson's ratio in the 13-direction
ν_{23} [-]	0.4	Poisson's ratio in the 23-direction

A second approach is also investigated, where the four shell plates are modelled without cohesive solid layers between. Instead, contacts are defined between the shell plates with the keyword *CONTACT_TIED_SURFACE_TO_SURFACE_OFFSET. This contact type works by allowing a set distance between two layers to create a contact with each other while also avoiding potential side effects from the combination of solid and shell layers. With the surfaces of the layers being placed close together, this contact type is suitable for the application. The fully integrated quadratic shell elements contain one node in each corner.

The final model is shown in Figure 3.2, displaying the cross-section of the plates and the four plates stacked on top of each other, connected by their surfaces. By using surface contacts, solid cohesive elements are not needed for the layers to behave as a single structure. This reduces computational cost by decreasing the number of elements in the model. In Figure 3.3, the four layers of the plate modelled in LS-DYNA are shown.

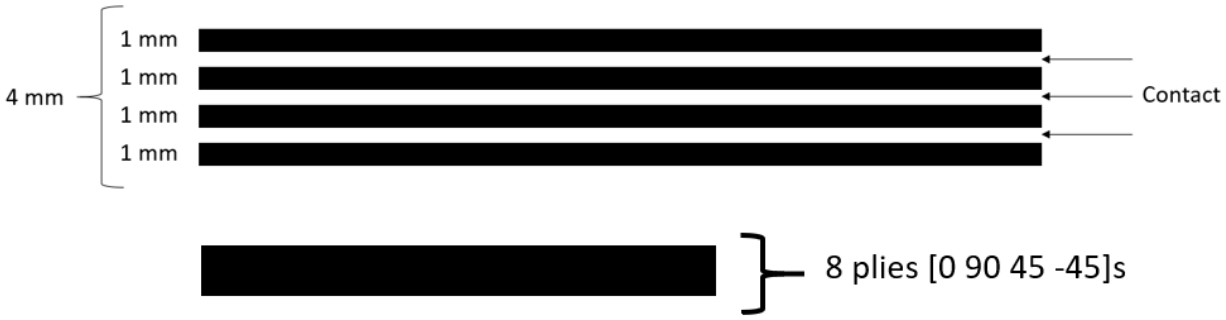

Figure 3.2: The cross section of the model with four layers, each containing 8 plies.

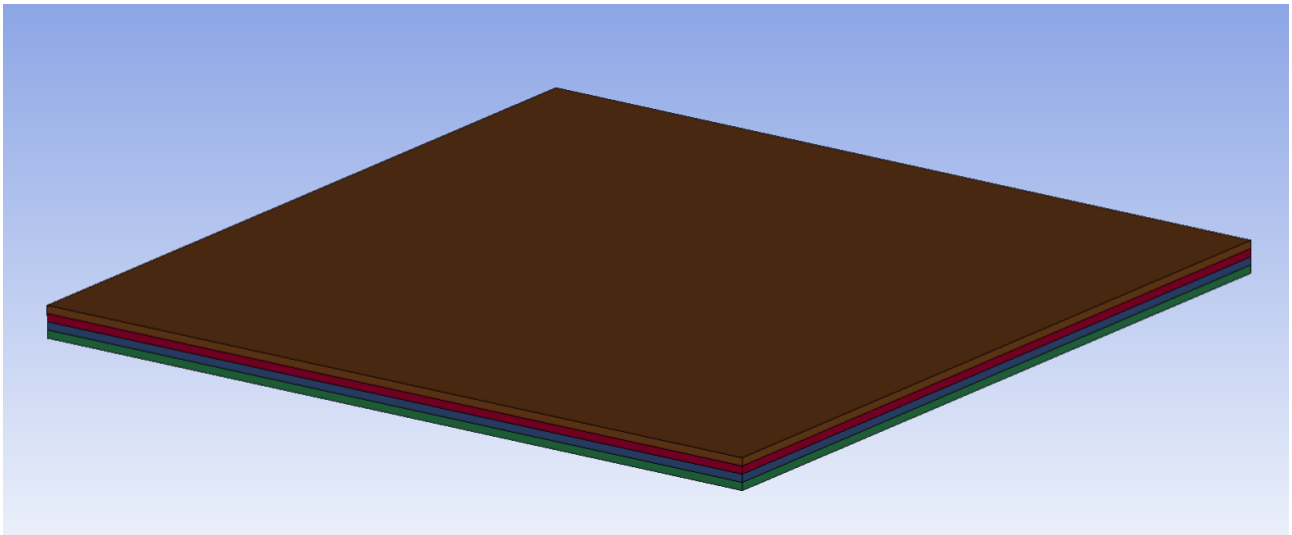

Figure 3.3: The composite model in LS-DYNA, displaying the stacking of the four element layers.

3.3 Lamb Wave Signal Definition

To define the excitation signal from the PZT transducers, some simplifications are made. The simplified excitation signal is defined by a prescribed time-dependent nodal displacement, designed to replicate the vibrations induced by the excitation. The signal is highly dependent on the material properties and the layup of the composite, and it is therefore not possible to use one signal for all materials. Thus, the signal must firstly be extracted from a dispersion curve obtained from the unique material properties of the composite.

3.3.1 Dispersion Curve

It is important to understand the dispersion characteristics of Lamb waves to be able to choose an appropriate excitation frequency. It is however complicated to solve the dispersion equations for multilayer composite materials due to quasi-isotropy, which means the material behaves nearly isotopically but still has directional dependence through the thickness. This is thus solved using The Dispersion Calculator [29] where the dispersion curve for the phase velocity is calculated for the A_0 wave mode, shown in Figure 3.4.

The thickness of the plate plays an important role when choosing the frequency for the A_0 Lamb wave mode, where thinner plates typically require a higher frequency. However, higher frequencies create complications with the simulation time, as the frequency is a factor when determining the minimum mesh size of the plate, explained in Section 3.4. A frequency of 100 kHz is thus chosen to accommodate the simulation time, although such a low frequency is typically used in thicker composites. This frequency, according to the dispersion curve in Figure 3.4, gives a phase velocity of 1521.15 m/s.

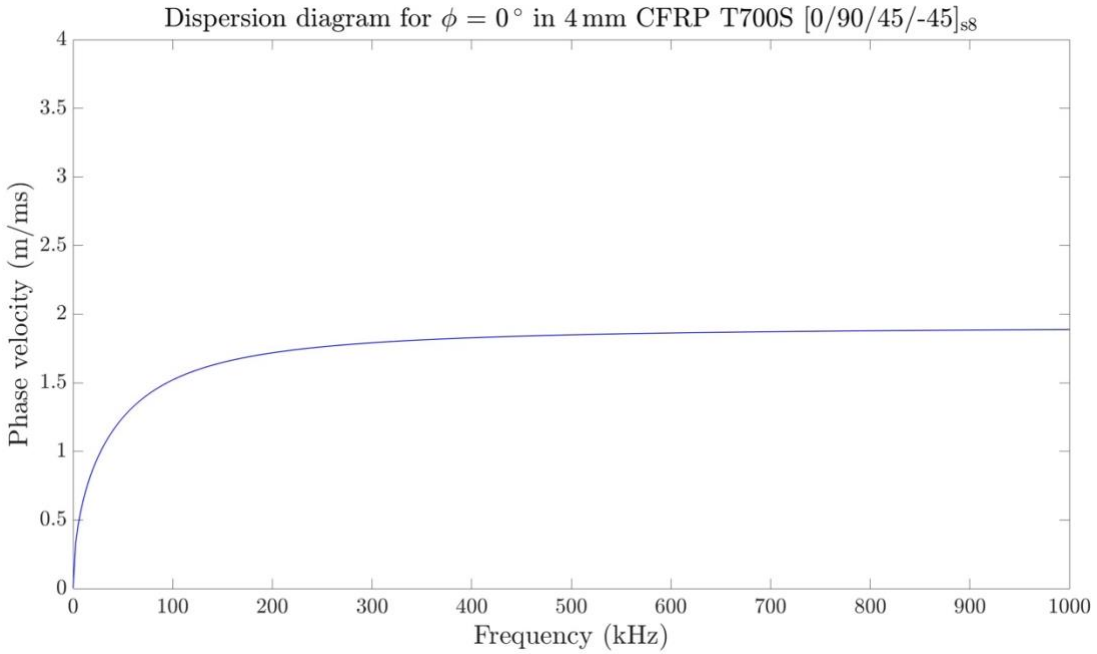

Figure 3.4: Dispersion curve of the T700S composite layup showing the phase velocity as a function of frequency.

3.3.2 Excitation Signal

Once the phase velocity is determined, the excitation signal can be obtained from the Dispersion Calculator, shown in Figure 3.5. Since the signal is a displacement rather than a voltage excitation, the value of the y-axis is in [nm] which corresponds to the through-thickness displacement. Moreover, a set propagation distance is defined as 50 mm to avoid reflections from the edges of the plate before the excitation signal has passed through the receiver node. The chosen excitation frequency of 100 kHz is stated as input as well as the number of cycles within the wave packet and the samples per cycle. Lastly, the window function that the signal shall pass through is defined, where the Hanning window function is chosen according to Section 2.3.3.

Figure 3.5 displays the excitation signal obtained from The Dispersion Calculator, with the number of cycles set to 5 and samples per cycle set to 10. The number of cycles determines the duration of the signal, while the samples per cycle specify the resolution, ensuring that each cycle is represented by 10 data points. This resolution enables a more accurate representation of wave propagation, capturing small details of the dispersion behavior within the specified duration.

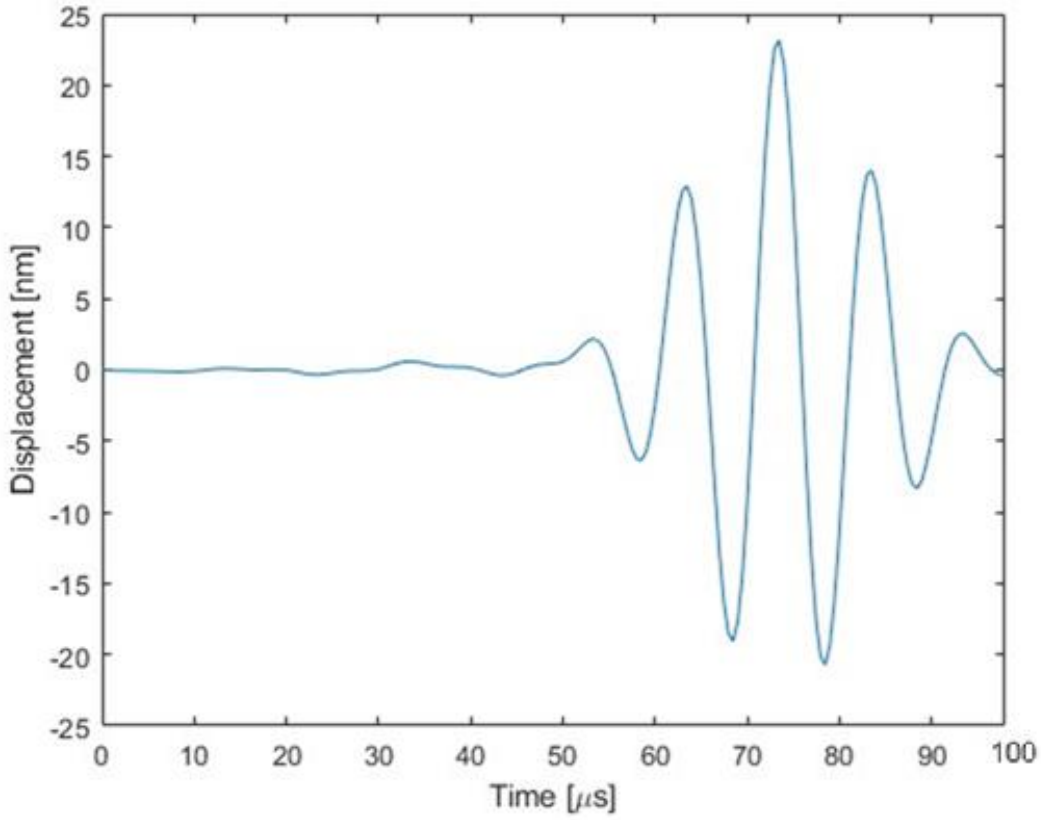

Figure 3.5: The excitation signal with the through-thickness displacement as a function of time passed through a Hanning window.

3.3.3 Nodal Displacement

The nodal displacement can now be assigned using the excitation signal from Section 3.3.2, which is applied through the *BOUNDARY_PRESCRIBED_MOTION_NODE keyword. A node on the top surface is selected as the excitation node, which will move in accordance with the excitation signal in Figure 3.5. The prescribed motion will oscillate with both negative and positive displacement along the z-axis, similar to the contraction and expansion of a PZT sensor in response to an electric signal.

3.4 Meshing

The element size depends on the wavelength, as previously stated in Section 2.4.1. With the chosen frequency of 100 kHz and the phase velocity of 1521.15 m/s, the wavelength becomes: λ = 15.12 mm. By considering at least 10 elements per wavelength, which is a common approach referred to in section 2.4.1, the critical element length becomes l_{crit} = 1.521 mm. However, a smaller maximum element size of 1.25 mm is selected to ensure accuracy, considering 12 elements per wavelength.

Using the maximum element size as an initial choice ensures basic resolution but does not ensure numerical accuracy for the specific application. A mesh convergence study is necessary to determine the optimal element size, minimizing mesh-induced errors such as wave dispersion and boundary reflection. The mesh convergence study also balances accuracy and computational cost. The timestep is initially set to an arbitrary value of 1 μs for the convergence study, but with the calculated time step presented in 3.4.1, the timestep is then changed to 0.1 μs and the simulations are conducted with this timestep. The duration of the excitation signal shown in Figure 3.5 is 100 μs. However, for the wave to fully propagate through the receiver nodes the simulation must be extended to 140 μs.

Figure 3.6 shows the nodal displacement in the receiver node for the different element sizes. The maximum difference between the element size of 0.3125 mm and 0.28 mm is less than 1% and convergence is considered to be reached. To optimize the computational time, the element size of 0.3125 mm is then selected. With this mesh size, the full model consists of 409600 elements with two translational- & three rotational degrees of freedom. The simulation runs in approximately 40-50 minutes on a high-performance laptop CPU with 24 cores.

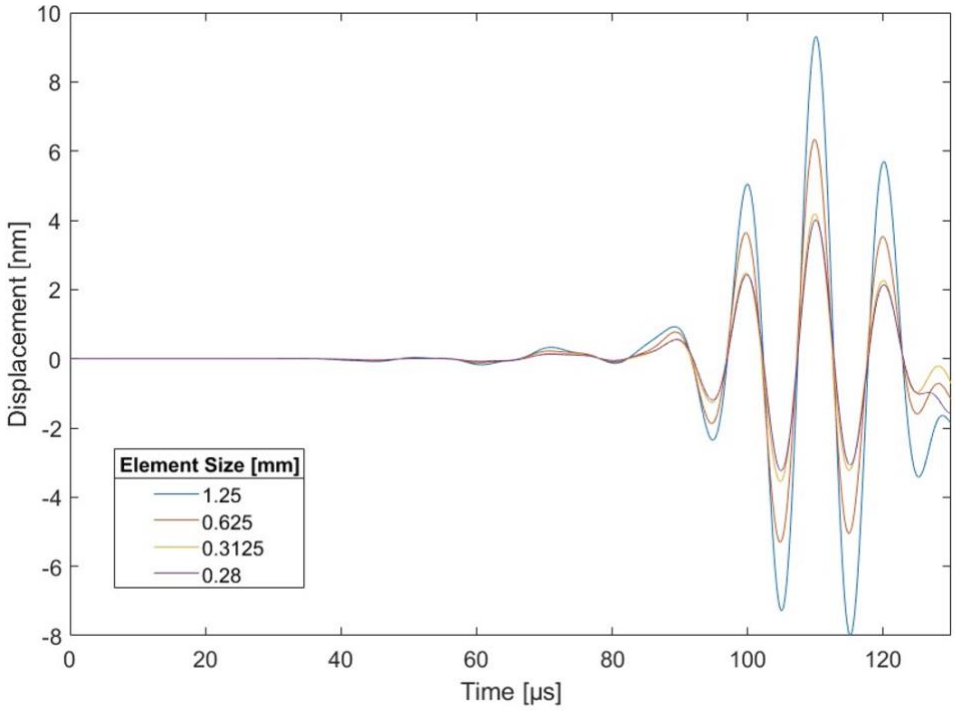

Figure 3.6: Mesh convergence study through assessment of the nodal displacement, showing a decrease in displacement for decreasing element size.

3.4.1 Timestep

In this explicit simulation, the CFL stability condition is used to determine the maximum allowed timestep. The selected element size using the mesh convergence study presented in Section 3.4.2 is 0.3125 mm. With the obtained phase velocity of 1521.15 m/s and the safety factor of $C_{max} = 0.5$, a timestep of 0.1 μs is obtained and implemented.

3.5 Boundary Conditions

Since the Lamb waves experience reflective behavior at boundaries such as plate edges, the boundary conditions may affect the capture of the signal at the receiver node. An investigation of the boundary conditions is thus conducted where two cases are investigated: clamped and simply supported along the edges of the plate. In the clamped case, displacements and rotations in and around the x-, y-, and z-direction are restricted while displacements in the z-direction are restricted in the simply supported case. For both cases the obtained element size of 0.3125 mm is used.

Figure 3.7 displays a comparison of the displacement in the receiver node in the two cases, showing that the reflection of the signal gets amplified for the clamped plate case. The signal before the reflection follows the behavior of the excitation curve up until 130 μs, meaning that both cases are appropriate depending on the size of the plate and the experimental setup. In this study, the size of the plate is relatively small while there are no requirements on the setup of the plate, which points to the choice of a simply supported plate being the most fitting since reflections are undesirable. The simply supported boundary condition will thus be used throughout the remainder of the report.

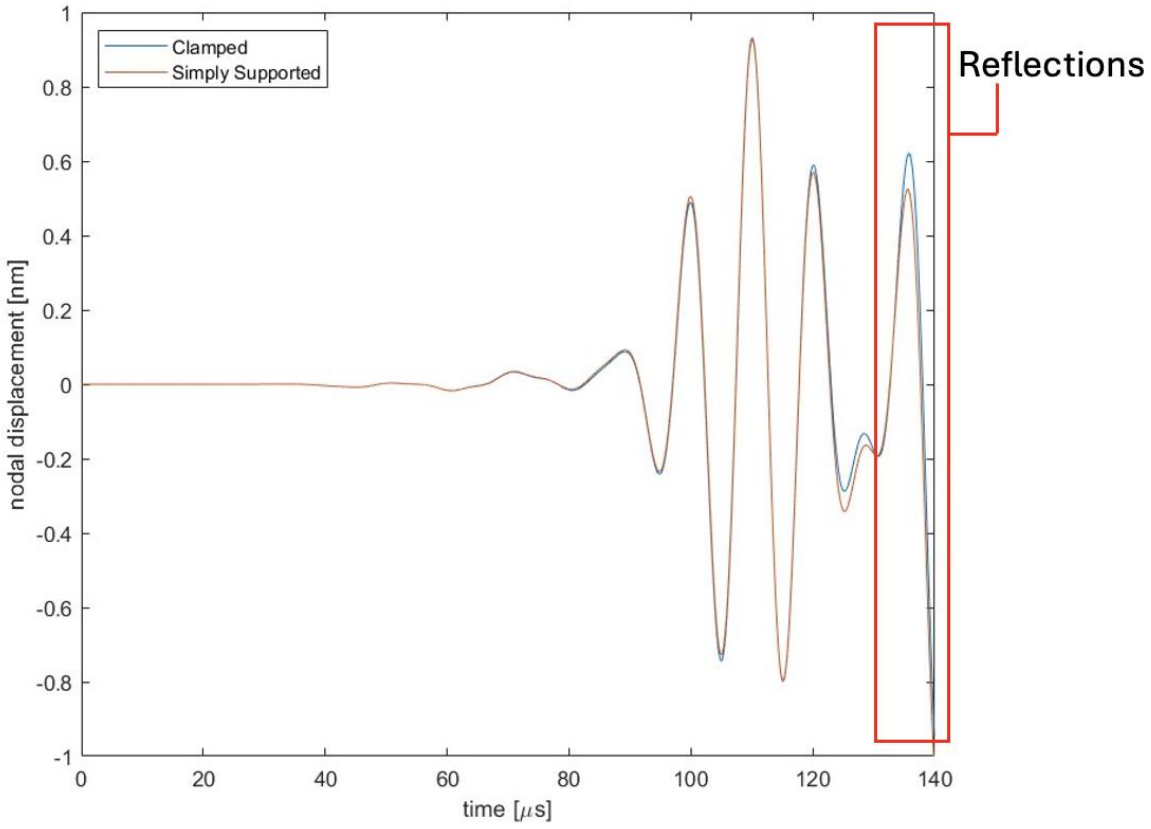

Figure 3.7: Comparison between the two boundary conditions investigated, showing a higher peak in amplitude from reflections in the clamped case.

3.6 Damage Modelling

To model defects like cracks and delaminations, the shared nodes between a few shell elements are detached for damage replication. If solid elements were to be used, it would

be possible to detach the nodes through the element thickness, simulating a transverse crack. However, the chosen element formulation restricts such damage modelling with the thin shells not having more than one node in the thickness direction. Instead, with the final model presented in 3.2.1, the cracks and delaminations must be modelled in the same plane.

Figure 3.8 shows the nodal and elemental detachments for the damage modelling. Since the contact is defined by the element surface in each layer, detaching these elements will result in lost contact at the detached area, simulating a delamination. The crack modelling is done by detaching a row of nodes in the same plane.

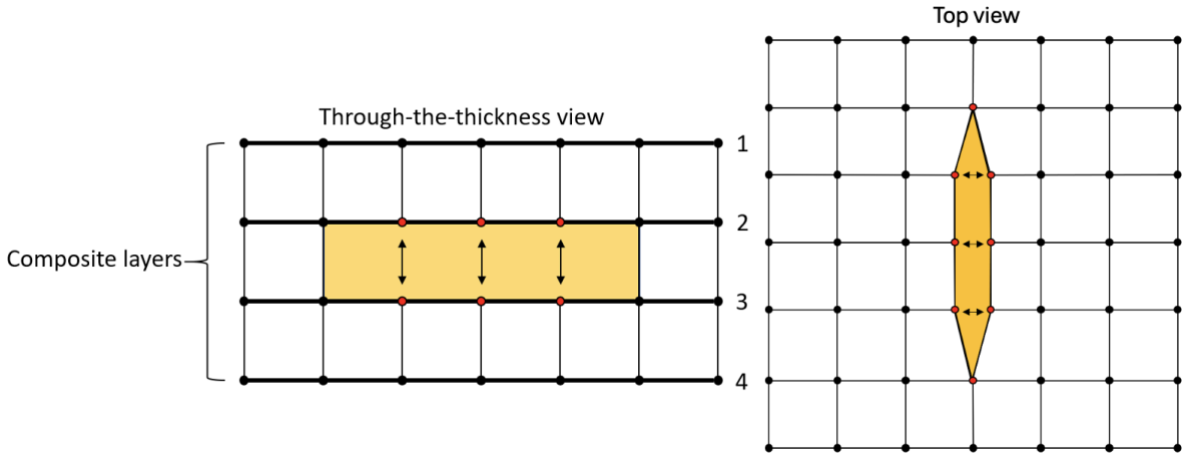

Figure 3.8: A) Delamination modelling. B) Crack modelling.

The minimum crack length and delamination area to be investigated is 6 mm, since this is the minimum size that can be detected in experimental studies [30]. The scale of the damage is thus modelled with this limitation in consideration. Figures 3.9 and 3.10 display the modelling of a crack and delamination in the second layer of the plate, i.e. between the 8th and 9th ply in the composite. The sizes of the damages are 6 mm in length for the crack and 36 mm^2 for the delaminated area, i.e. the crack size squared. The squared region in Figure 3.10 is the total area where the plies lose surface contact.

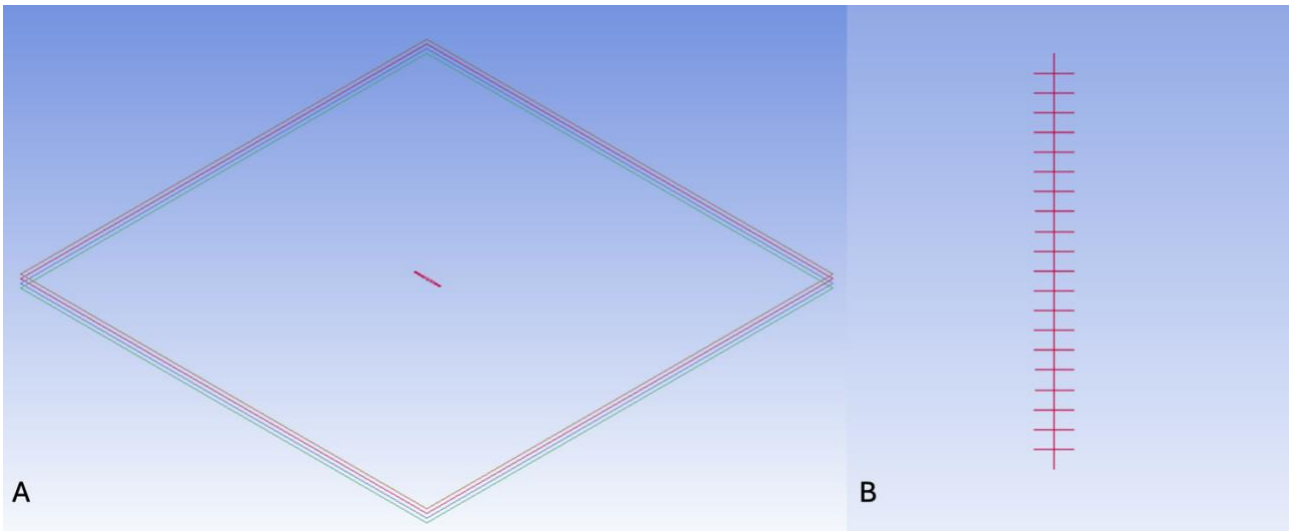

Figure 3.9: A) 6 mm crack in the second plate layer, i.e. between ply 8 and 9 in the composite. B) Closeup on the crack.

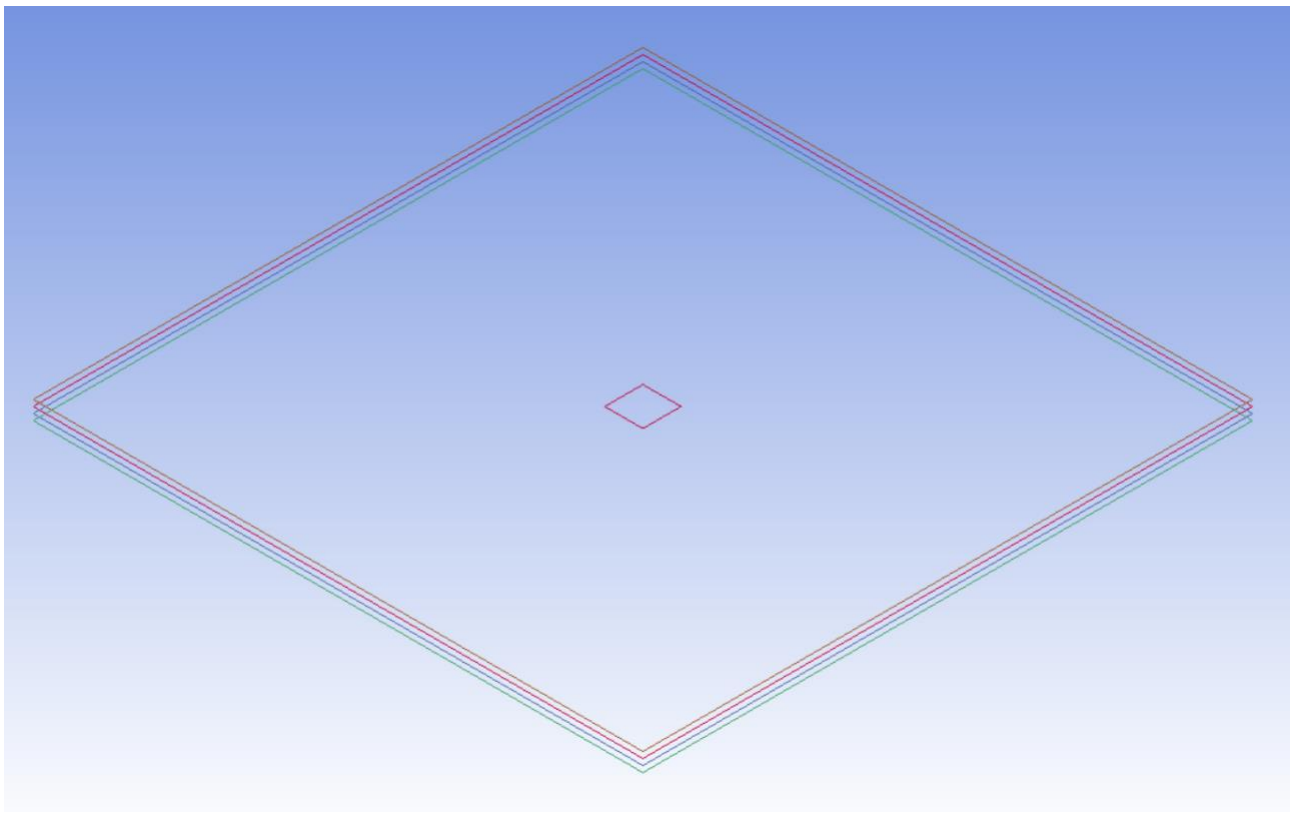

Figure 3.10: Delamination modelled in the second layer of the model, i.e. between ply 8 and 9 in the composite.

3.7 Sensor Placement

Since the location of the damage is unknown in real-life applications, various placements of the simulated PZT sensors will be evaluated to be able to locate the damage. In this study, the placement of 8 sensors will be assessed, i.e. 8 nodes, where one of the sensors will act as signal excitor and the remaining seven sensors will act as receivers. To simplify this, node 2 is chosen as the excitor for the localization investigation. A schematic of the sensor placements is shown in Figure 3.11. The scattered placement of the sensors allows for assessment of different locations and types of damages.

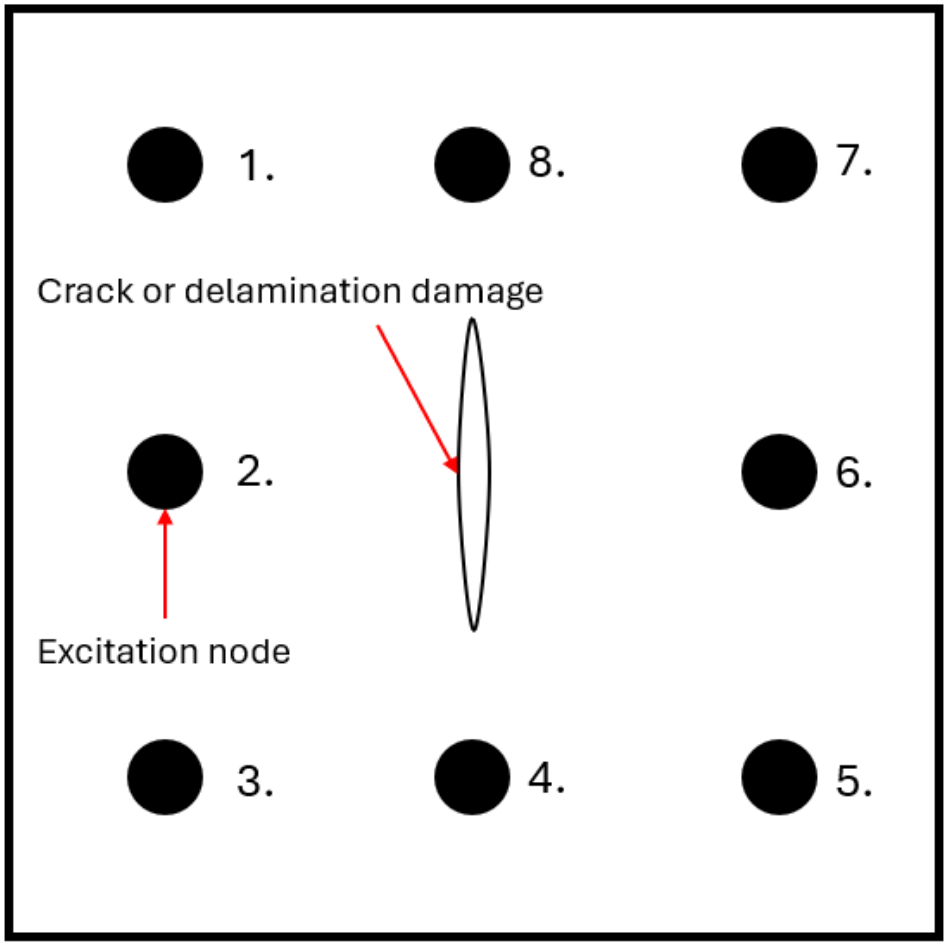

Figure 3.11: Sensors placed across the plate for localization evaluation.

Another sensor placement is also evaluated, shown in Figure 3.12, where another 9 nodes are defined as receptors. This placement is done to be able to investigate a temporal difference of the wave as it propagates over the plate and the damaged region. The temporal difference is calculated according to:

$$\Delta t = t_{damaged,i} - t_{intact,i}, i = 2, \dots, 10$$

where $t_{intact,i}$ is the time of arrival for the wave at node i in the intact plate, and $t_{damaged,i}$ the time of arrival at node i in the damaged plate. Here, time of arrival is obtained from the timestep where the receiver node reaches the maximum amplitude value, i.e. the largest amplitude peak. The investigation is conducted to demonstrate how the wave scatters as it propagates over the damaged region.

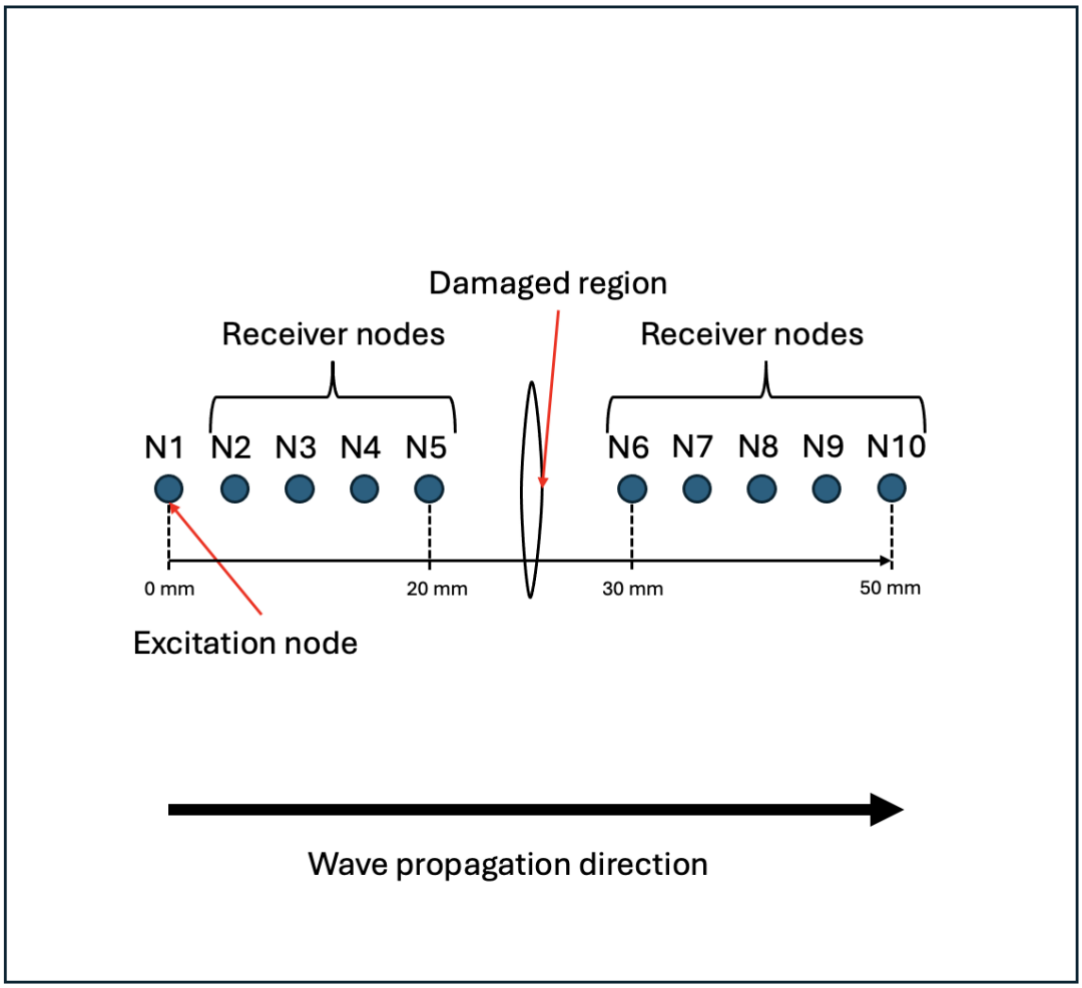

Figure 3.12: Setup for the propagation time over damage region investigation.

3.8 Damage Localization

The sensor placement explained in Figure 3.11 will be used to determine the location of the damage. To perform this investigation in LS-DYNA, node 2 will initially act as the excitation node, and the remaining nodes as receivers. A simple test can be performed to determine the location, where node 2 is excited both for an intact and damaged plate model. In case I, the placement of the damage is in the middle of the plate between node 2 & 6, in the second layer. In case II, the placement of the damage is changed to a location between node 2 & 8. The placement of the damages in the two cases are shown in Figure 3.13. The amplitudes of the through-the-thickness displacements of the damaged and intact nodes are then subtracted according to:

$$\Delta a = a_{intact} - a_{damaged}$$

where Δa is the difference in amplitude in the same node, at a given time, between the damaged and intact plate. When using multiple receiver sensors for damage localization, analyzing amplitude differences enables a more straightforward assessment of the impact from damages compared to a temporal difference, as it is easier to visualize. In theory, the damaged plate should give a lower amplitude compared to the intact plate, due to the scattering and reflections of the Lamb wave previously stated in Section 2.2.

Therefore, the difference should be more apparent at the node at which the damage is in the wave propagation path, i.e. node 6 for case I and node 8 for case II.

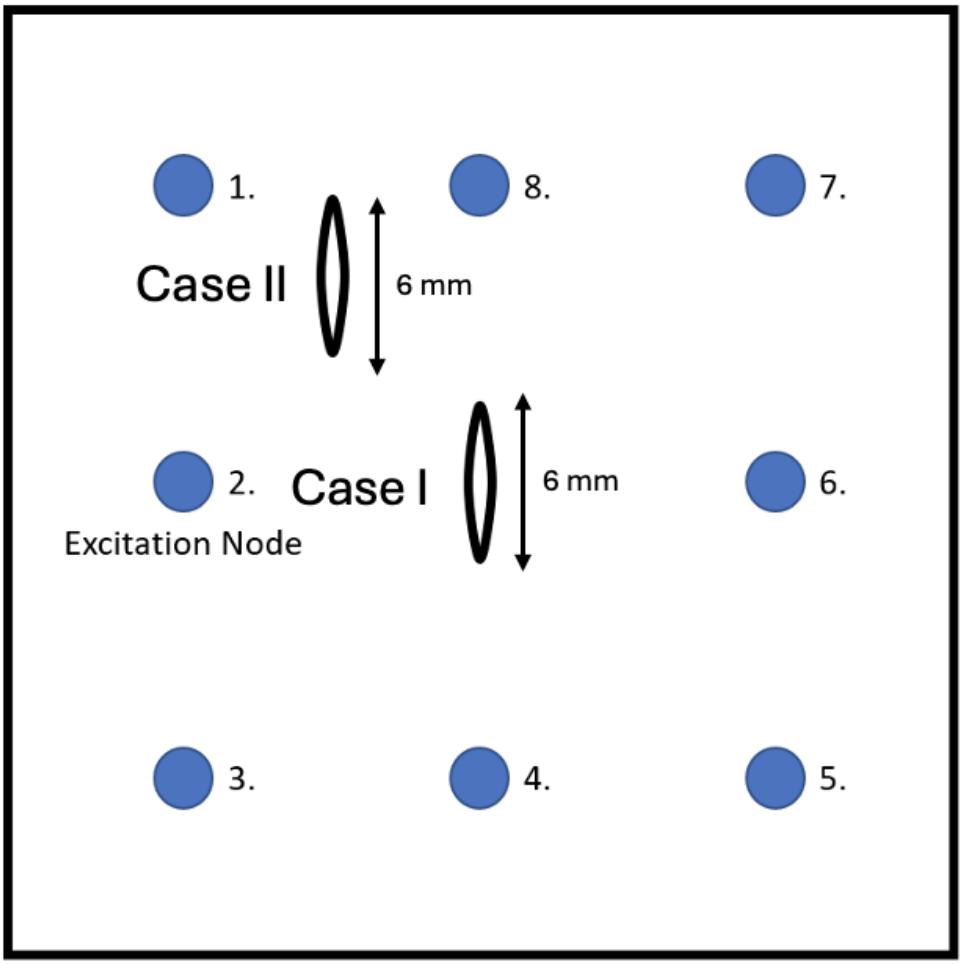

Figure 3.13: The two placements for the crack, between node 2 & 6 in the first case and between node 2 & 8 in the second case.

3.9 Model Variations

To investigate the robustness of the model's ability to detect damage, a study of model variations is performed. In the study, the thickness of the plate, frequency of the excitation signal, and material properties are altered to get an understanding of what impact this will have on the results. Also, the presence of bolt holes is investigated.

3.9.1 Bolt Holes

A common method for joining composite structures is mechanical fastening such as bolting. However, introducing bolt holes into the composite structure can significantly affect the wave propagation. The Lamb waves can be scattered and reflected by bolt holes, similar to how they react to a damage.
Since the locations of the bolt holes in the structure are known in advance, and the method relies on comparing a damaged structure to an intact one, it is not essential to fully characterize the effects of the bolt holes on wave propagation. Instead, a more critical aspect to investigate is whether the bolt holes reflect such a significant portion of

the Lamb waves that reflections from actual damage might be masked by noise, making them more difficult to detect.

To analyze this issue, the plate is modelled with a centrally placed hole. To accurately capture the wave propagation around the hole while ensuring numerical stability, a meshing technique known as the Butterfly Mesh is applied around the hole. This technique is beneficial when a smooth transition from fine to coarse elements is needed to maintain numerical stability. Since wave propagation is sensitive to changes in the model, an abrupt mesh transition can disrupt the wave behavior and lead to inaccurate results. The edge around the hole is simply supported, i.e. locked in the z-axis degree of freedom. The model will be subjected to $6x6\ mm^2$ delaminations around the plate to see whether they can still be detected when the bolt hole is present. The model is displayed in Figure 3.14. A closeup of the mesh around the bolt hole is shown in Figure 3.15.

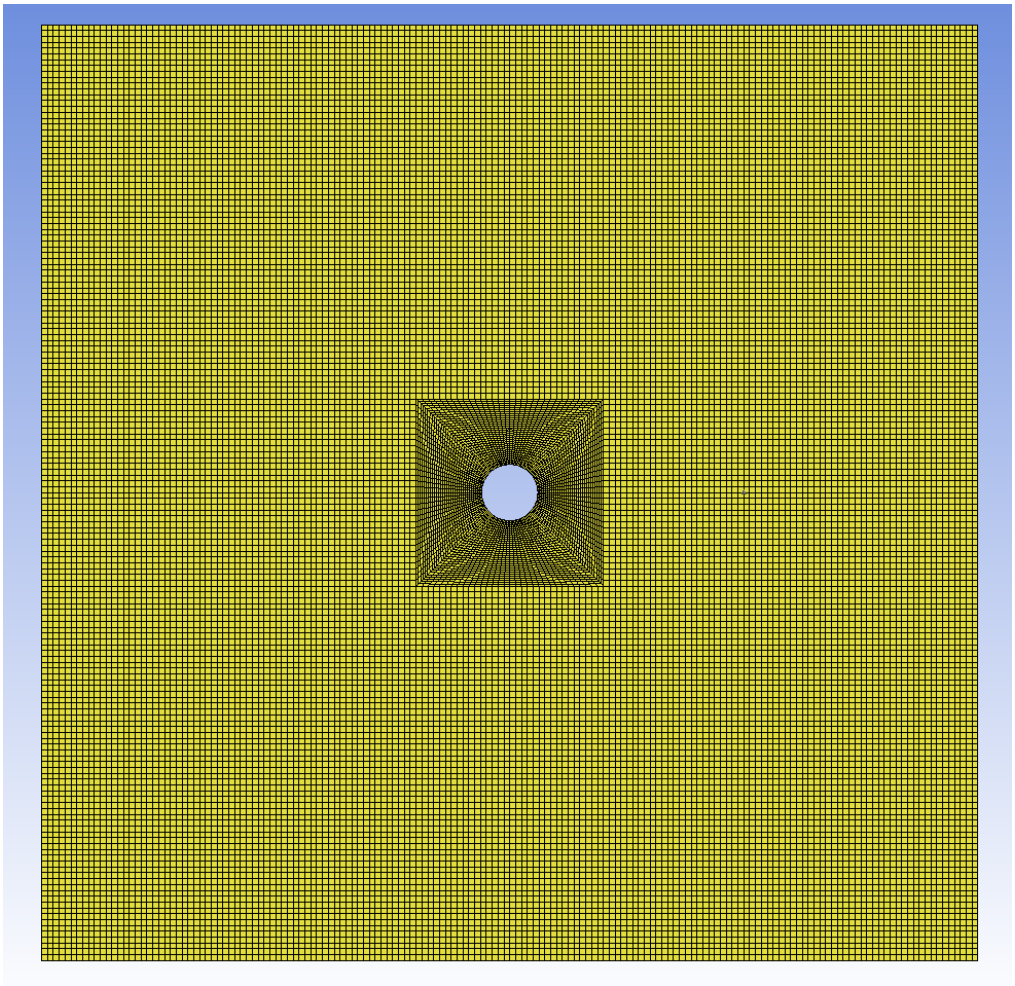

Figure 3.14: Composite plate model with a butterfly meshing approach to capture the bolt hole.

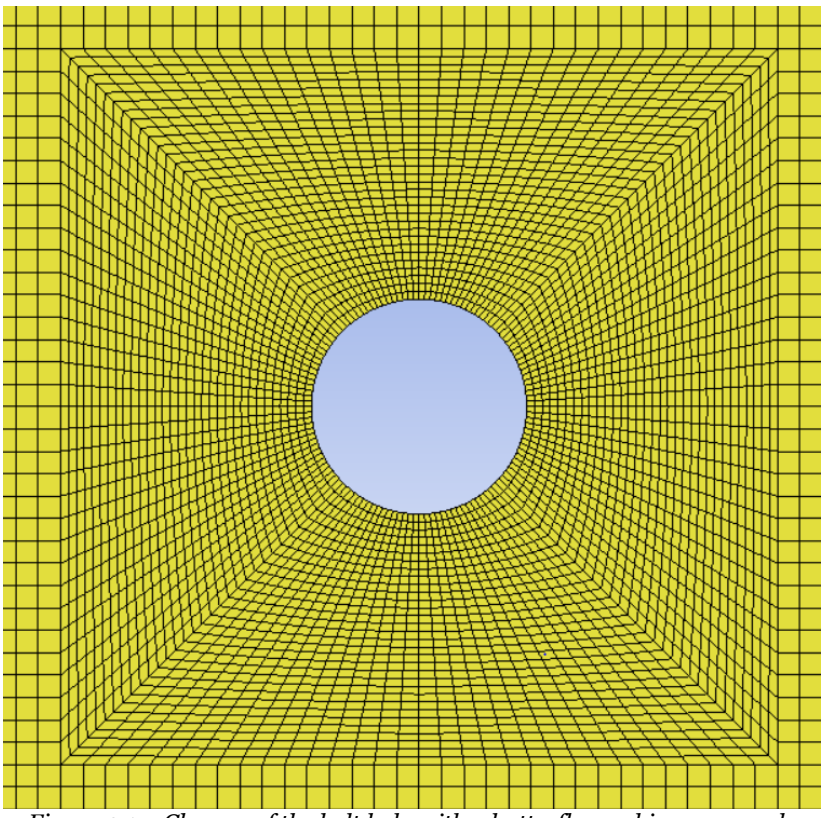

Figure 3.15: Closeup of the bolt hole with a butterfly meshing approach.

3.9.2 Thickness, Frequency & Input Variation

In the thickness study, four different thicknesses are investigated: 2, 4, 6, and 8 mm respectively, which in turn leads to more or fewer plies in the composite layup, presented in Table 3.2. An intact and damaged model is then compared, where the damage is placed in the center ply of each model to get an understanding of how deep inside the composite plate damages can be detected. The damage modelled in this investigation is a 6 mm crack.

Table 3.2: Investigation of different thicknesses and the number of plies each thickness corresponds to.

Thickness [mm]	Number of plies
2	16
4	32
6	48
8	64

When performing the frequency study, four different frequencies are investigated: 100, 125, 150, and 200 kHz respectively. This study is performed to get an understanding of which frequencies are optimal for damage detection, as different frequencies might interact differently with specific types of damages. Lower frequencies are typically used for thicker plates since they have a higher thickness penetration, while higher frequencies are used for thinner plates and can be more sensitive to smaller defects, as previously mentioned in Section 3.3.1. New excitation signals are thus defined for the frequencies of 125, 150, and 200 kHz, shown in Figure 3.16 together with the previously used 100 kHz excitation signal.

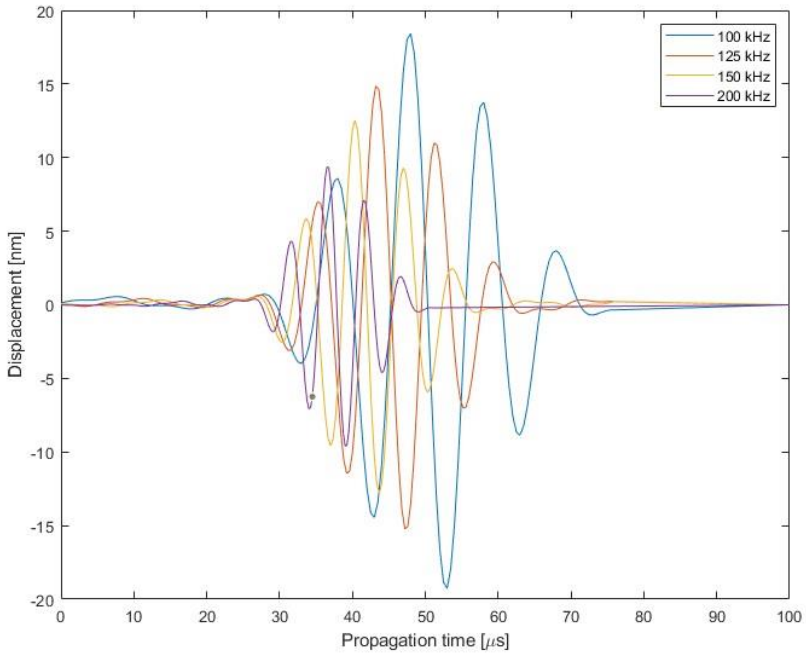

Figure 3.16: The four excitation signals used for the frequency study.

The final model variation investigation is to degrade the material properties of the composite. This is performed to investigate an alternative damage modelling technique which might be beneficial in terms of computational efficiency. The material degradation is done in two ways, where the first approach is to model the entire composite plate as one layer of shell elements and degrade some of the plies in the *PART_COMPOSITE keyword. Modelling the damage by degrading entire plies enables the use of a one shell layer formulation, as only one part is needed. In the first case, two of the middle plies are degraded by 20%, where the material properties are listed in Table 3.3. In the second case, four plies in the middle of the structure are degraded with 20%.

The second approach is to degrade a region in one layer of the plate to investigate if this approach can be used to model a delamination instead of detaching nodes in a layer. The material properties that are degraded are the stiffnesses E_1, E_2, and E_3 as well as the shear modulus G_{12}, G_{13}, and G_{23} according to Table 3.3, since these properties are typically affected when a delamination is present in the composite.

Table 3.3: Degraded material properties for two cases of degradation

Material properties	Intact	20% degraded	40% degraded
E_1	139 GPa	111.2 GPa	83.4 GPa
E_2	8.5 GPa	6.8 GPa	5.1 GPa
E_3	8.5 GPa	6.8 GPa	5.1 GPa
G_{12}	4.2 GPa	3.36 GPa	2.52 GPa
G_{13}	4.2 GPa	3.36 GPa	2.52 GPa
G_{23}	2.2 GPa	1.76 GPa	1.32 GPa

4 Results & Discussion

In this chapter, the results of the implementation of the methodology will be presented and discussed.

4.1 Damage Detection

To answer the research question about how numerical simulations of Lamb wave propagation can be applied to detect damages in composite materials, the damaged plate is compared to an intact plate. The damaged plate contains a 6 mm crack on the top ply in the center of the plate. Figure 4.1 presents a comparison of velocity contour plots for the intact and damaged plate at three timesteps, illustrating how the crack disrupts the wave propagation path. This can be seen in Figure 4.2, where the difference between the intact and damaged plates shows a temporal delay and a decrease in amplitude for the damaged plate.

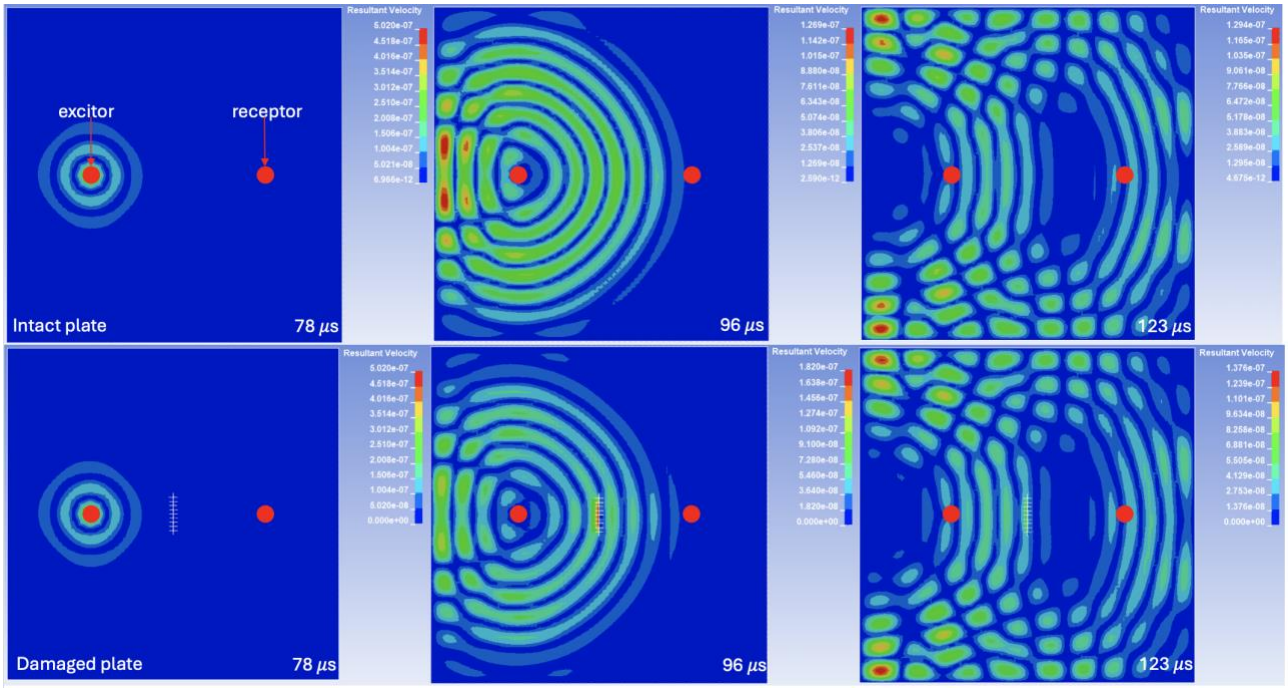

Figure 4.1: Velocity contour plot showing the smooth propagation over the intact plate, compared to the damaged plate where the damage disrupts the wave.

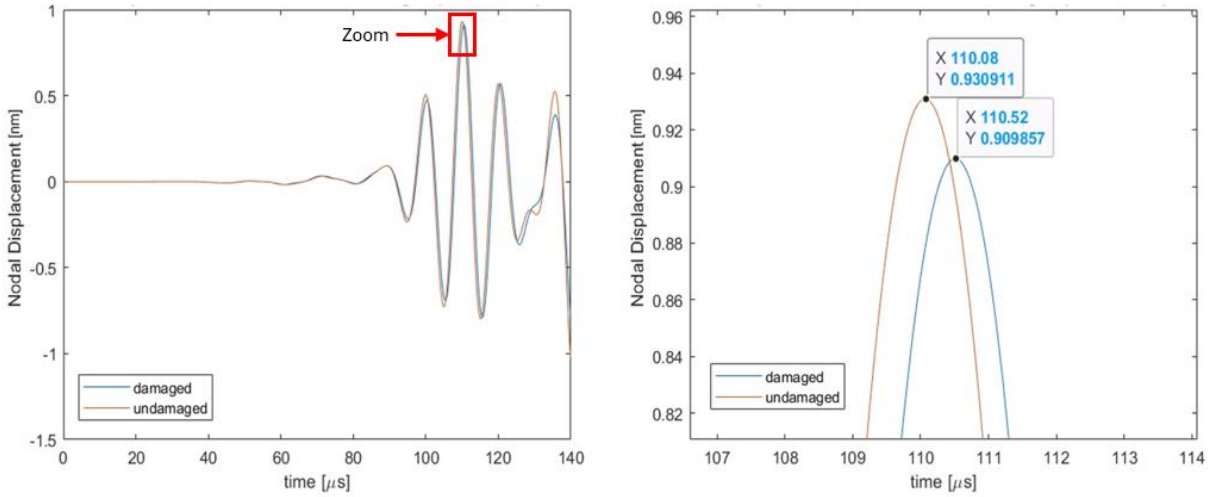

Figure 4.2: A) Comparison between damaged/undamaged plate, indicating a temporal delay in the damaged plate and an amplitude decrease. B) A closeup of the amplitude difference.

The sensor placement in Figure 3.12, evaluated to determine which sensors experience a time difference, shows that the time difference increases at a propagation distance of 20 mm. As seen in Figure 4.3, the time delay occurs between 20 mm and 30 mm, which is where the crack is located. This confirms that the crack is the cause of the time delay detected by the receiver sensor. The markers represent the receiver nodes, where the first mark at zero propagation distance is the excitor node.

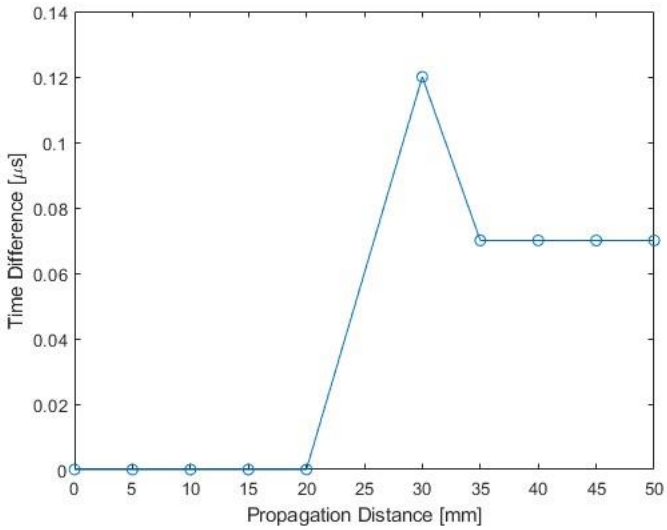

Figure 4.3: Time difference as a function of propagation distance from the excitor to the final receiver N10.

The comparisons show that it is possible to detect damage using Lamb Wave propagation. As seen in Figure 4.2, the receiver node exhibits a difference in amplitude compared to an intact plate. It is also seen from the velocity contour plot in Figure 4.1 that the damaged area experiences a change in velocity, i.e. the wave speed is decreased when the wave propagates over the crack. This results in a temporal delay seen at the receiver node.

4.2 Damage Localization

For the damage localization, a crack is placed in two different locations as seen in Figure 4.4. The amplitude readings from the seven sensors in the damaged plate are then extracted and subtracted from the readings in the intact plate, also shown in Figure 4.4 which shows the results from the first location, i.e. damage located between node 2 & 6. This investigation show that the amplitude difference is greatest for the nodes directly behind the damage, with node 6 having the largest difference between the intact and damaged plate. It can also be noted that node 5 & 7 both exhibit a larger difference, indicating that the wave scatters and reflects off the damage before it reaches these nodes, resulting in a larger amplitude difference.

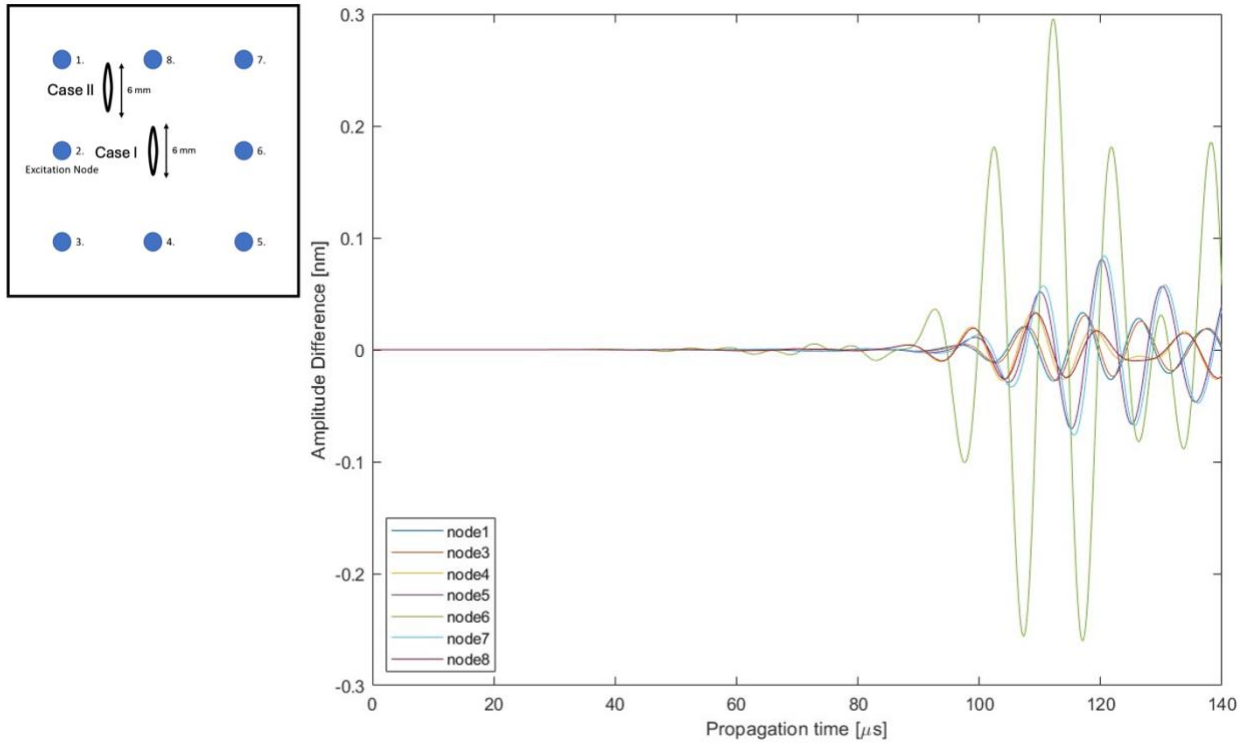

Figure 4.4: Amplitude difference between the intact and damage simulations for case I, showing a larger difference for node 6 which is behind the damaged region.

When the placement is changed to the second location, between node 2 & 8, the same pattern emerges, shown in Figure 4.5, as node 8 shows the largest difference in amplitude with node 1 & 7 having similar amplitude differences as in the first location investigation.

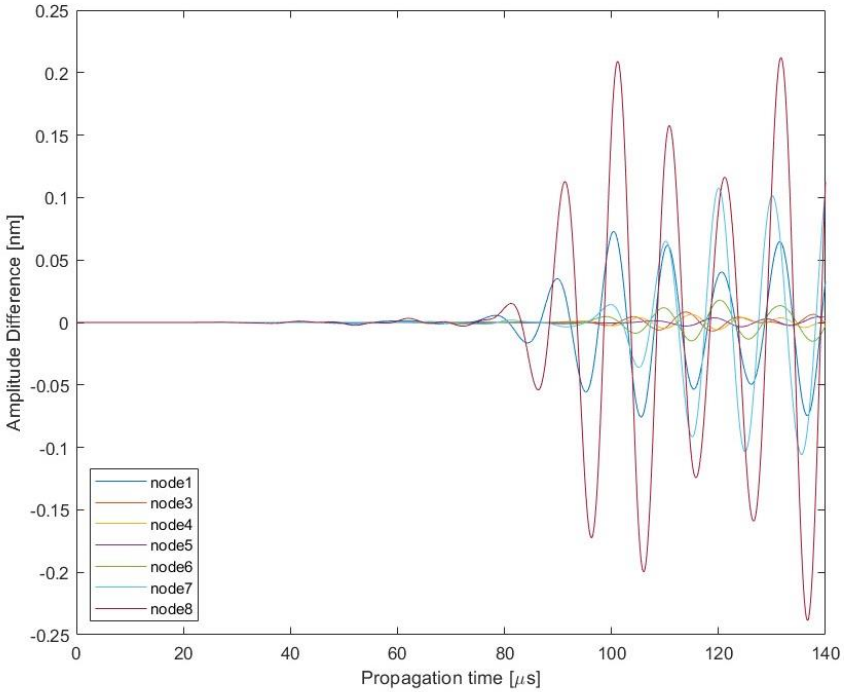

Figure 4.5: The amplitude difference for the second damage location for case II, showing a larger amplitude difference for node 8.

These results suggest that analyzing which sensor experiences the largest amplitude difference can provide insight into the location of the damage. With this method, the approximate location of the damage can be determined. By increasing the number of sensors, a more detailed triangulation can be achieved, which is especially useful for larger structures.

Now, with a reliable localization method for a single damage, the next approach is to determine whether it can be used for multiple damages. With the same sensor placement as before, the two cases in Figure 4.6 are examined. In case I there are two vertical cracks, one located between the excitation node and node 6, and the other between the excitation node and node 8. The graphs in Figure 4.7 show a similar result to the previous localization test where only one crack was present. In case I, nodes 8 & 6 exhibit the largest amplitude differences, since the paths between the excitation node and both these nodes are directly affected by a crack. Furthermore, node 7 exhibits a large amplitude difference since this node is partly affected by the two cracks even though this node is not directly behind any cracks.

In case II, the cracks are diagonal to investigate if crack orientation has any impact on the amplitude difference. In this case, the cracks interfere with the wave path between the excitation node and nodes 4 & 8. The results for case II show good agreement with the previous tests, as node 4 & 8, which are behind the cracks, exhibit the largest amplitude difference.

These results show that localization of a crack is possible. By analyzing which nodes experience the largest amplitude difference, the location of the crack can be triangulated. With more sensors used on the structure, a more detailed localization can be achieved.

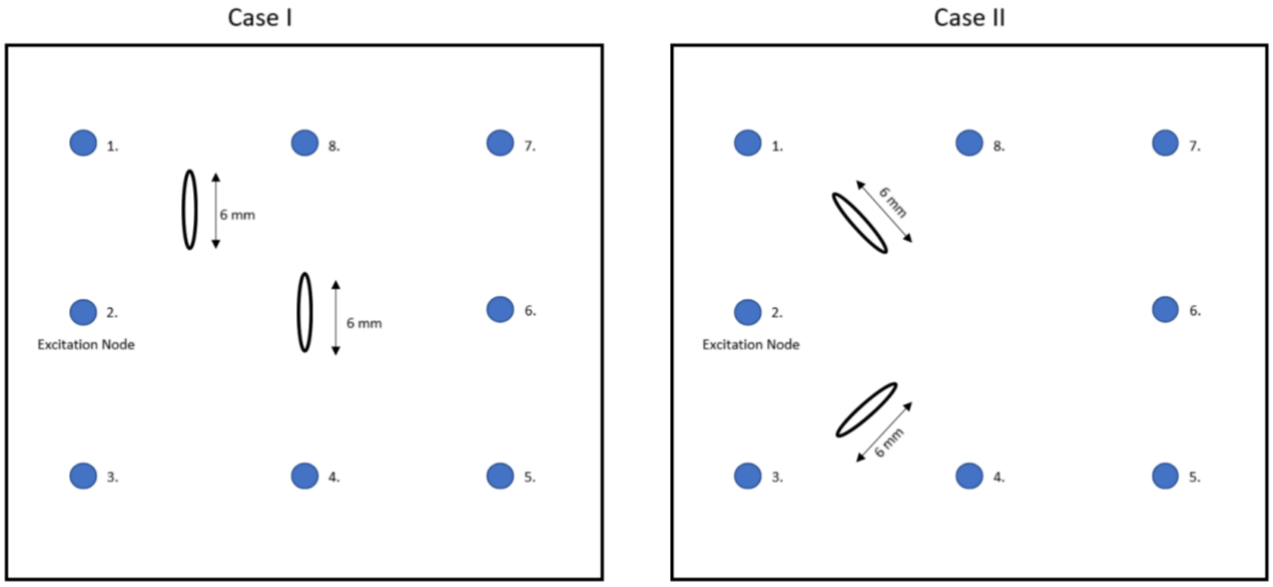

Figure 4.6: Illustration of the crack placement for cases I & II. All cracks have a length of 6 mm.

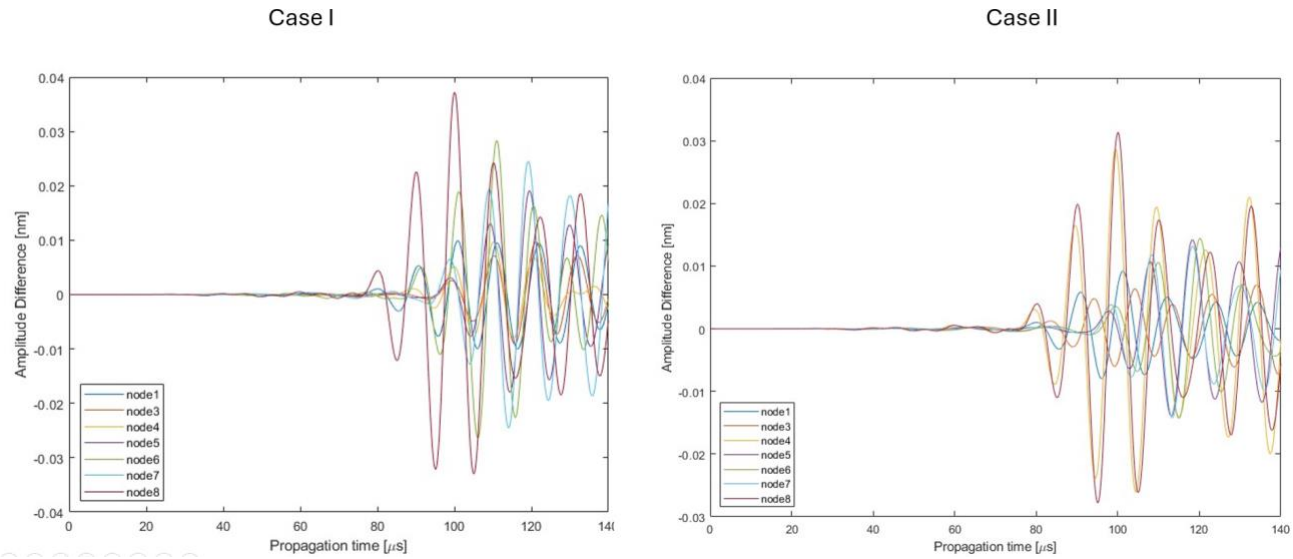

Figure 4.7: The amplitude difference for damage case I & II, showing a larger difference for the nodes behind the cracks.

The localization tests showed that it is possible to locate a crack with the use of multiple sensors. The next test investigates whether it is possible to also characterize the damage using the same method, i.e. by identifying differences in amplitude depending on the damage mode present. A sketch of the damage placement is shown in Figure 4.8. Both cases include a delamination and a crack at the same location. However, in case IV, the crack is 6 times larger than in case III.

The results for these two cases are shown in Figure 4.9, again displaying the amplitude difference in displacement over time for all the receiver nodes. In case III, the amplitude difference for node 8, which path is blocked by the delamination, is marginally higher than for node 4 which is behind the crack. In this case node 7 also exhibits a larger

amplitude difference than node 4, even though its path is not directly blocked by the delamination.

In case IV, which includes the larger crack, the amplitude difference at node 4 is greater than for case III, indicating that a larger crack has a more significant impact on the wave. However, the amplitude difference at node 8 remains the largest, suggests that the delamination has a greater impact on the wave propagation than even a large crack.

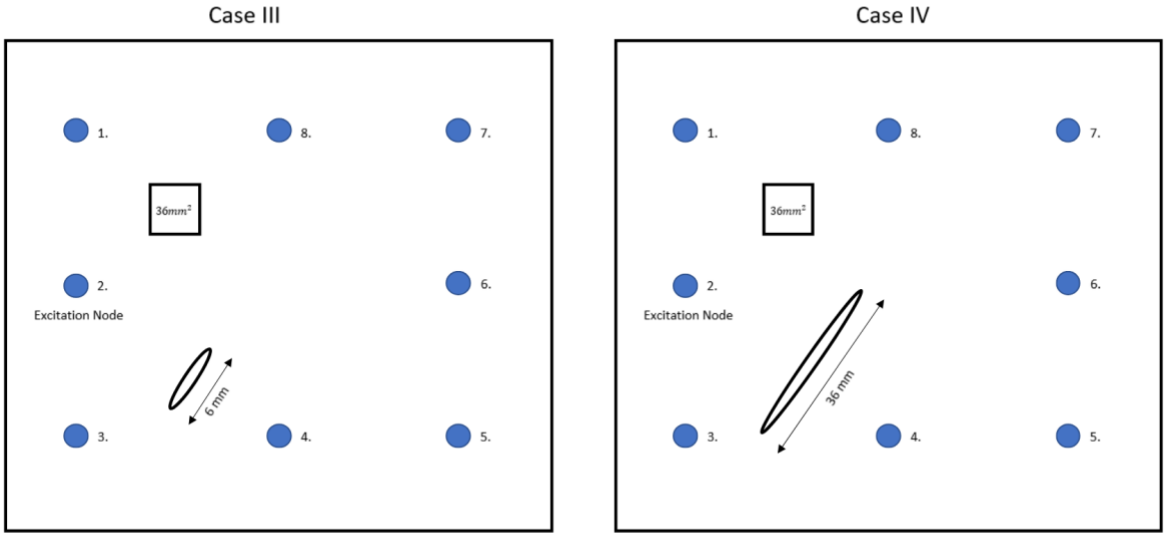

Figure 4.8: Illustration of the crack & delamination placement for cases III & IV, the delamination has an area of 36 mm². In case IV the crack is 6 times the length of the crack in case III.

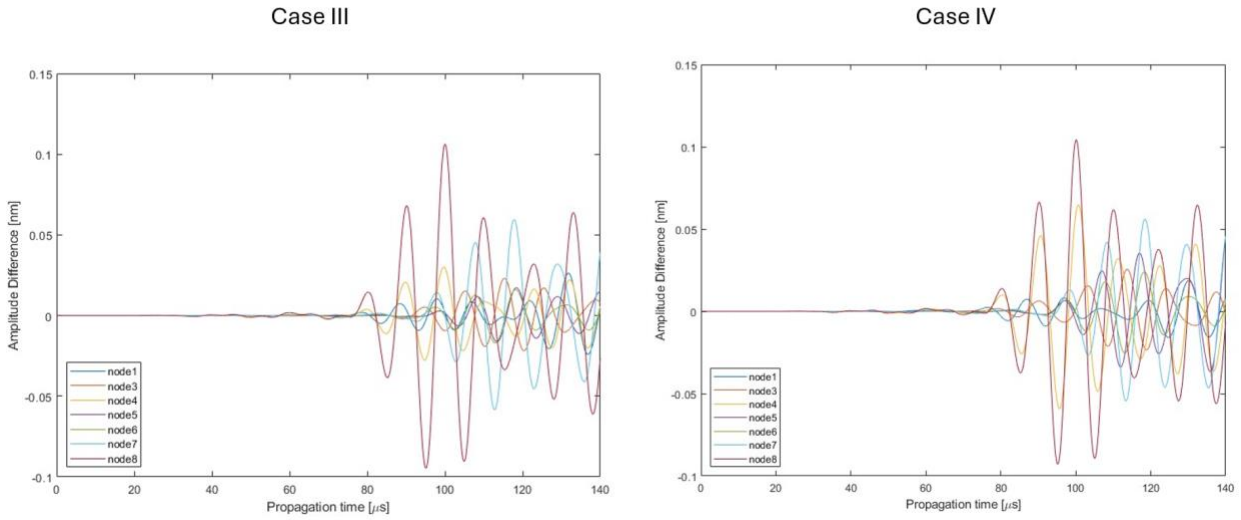

Figure 4.9: The amplitude difference for damage cases III & IV. The node behind the delamination exhibits a higher difference in amplitude than the node behind the crack, even when the crack is 6 times longer.

To summarize this result, characterizing the damage mode present might be possible considering the significant difference in amplitude if a delamination is present compared

to a crack. By simulating more cases, it might be possible to find a pattern in the amplitude differences and the different damage modes.

4.3 Delamination Bolt Holes

By applying the excitation to the same node as previous simulations, the velocity contour plot shown in Figure 4.10 is obtained, illustrating the wave propagation across the plate. The wave behavior is not significantly affected by the change in mesh, thus validating the use of the Butterfly Meshing approach.

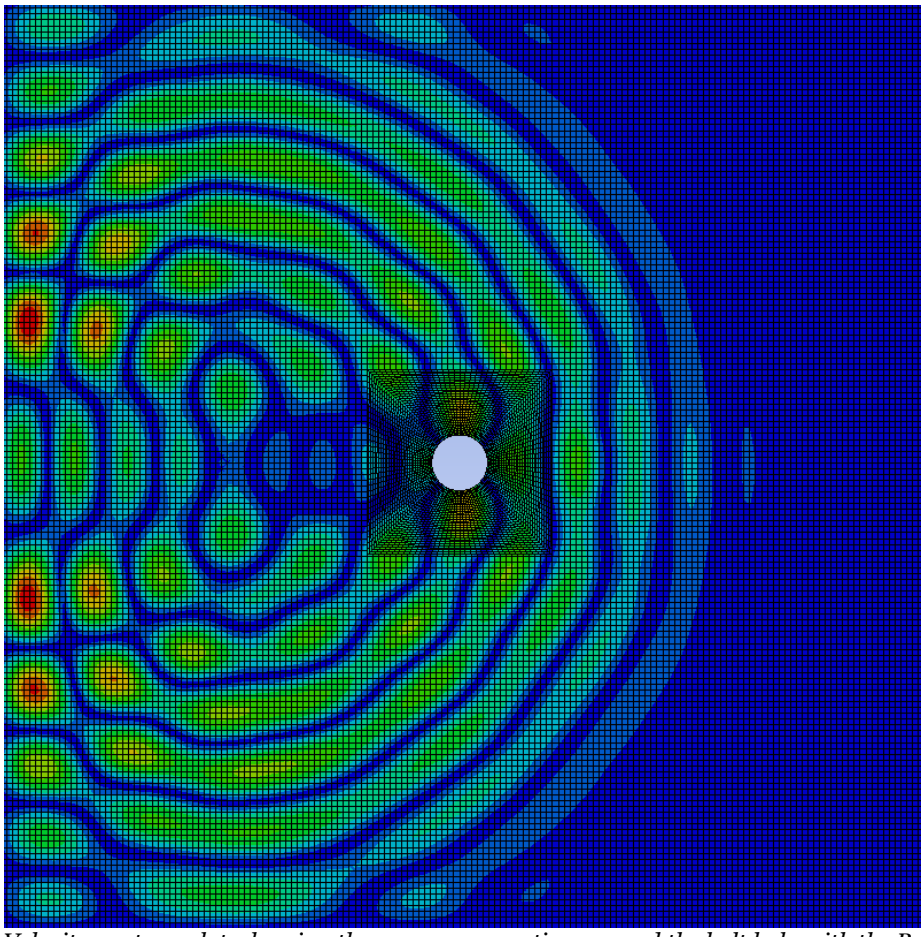

Figure 4.10: Velocity contour plot, showing the wave propagation around the bolt hole with the Butterfly mesh.

This investigation is conducted by changing the location of a delamination to three different positions, as seen in Figure 4.11. The results are obtained at the receiver node located on the opposite side of the bolt hole, with the goal of determining whether delaminations can still be detected when the hole is present.

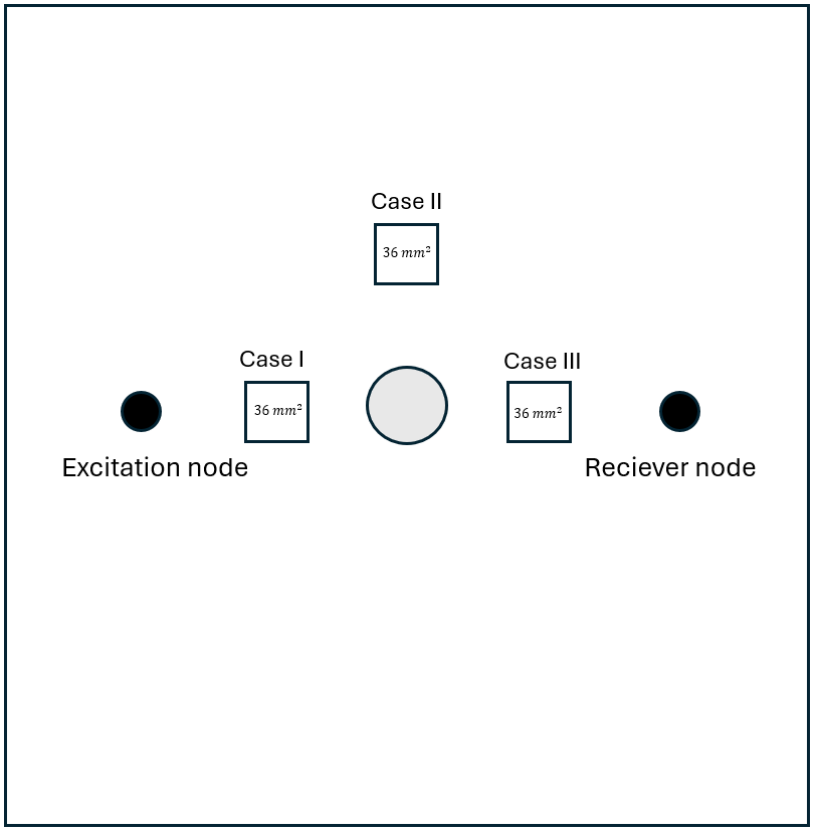

Figure 4.11: Illustration of the model containing a bolt hole with three different delamination cases.

Figure 4.12 displays the results for the three delamination cases together with an intact plate. The results indicate a clear difference between the intact plate and the three delamination cases. The most noticeable differences are observed in cases I and III, as these delaminations directly interfere with the wave path between the excitor and the receiver. Case II also shows a slight variation in amplitude and time delay, suggesting that this delamination is detectable as well. By using additional sensors around the plate, delaminations could potentially be detected even in the presence of multiple bolt holes.

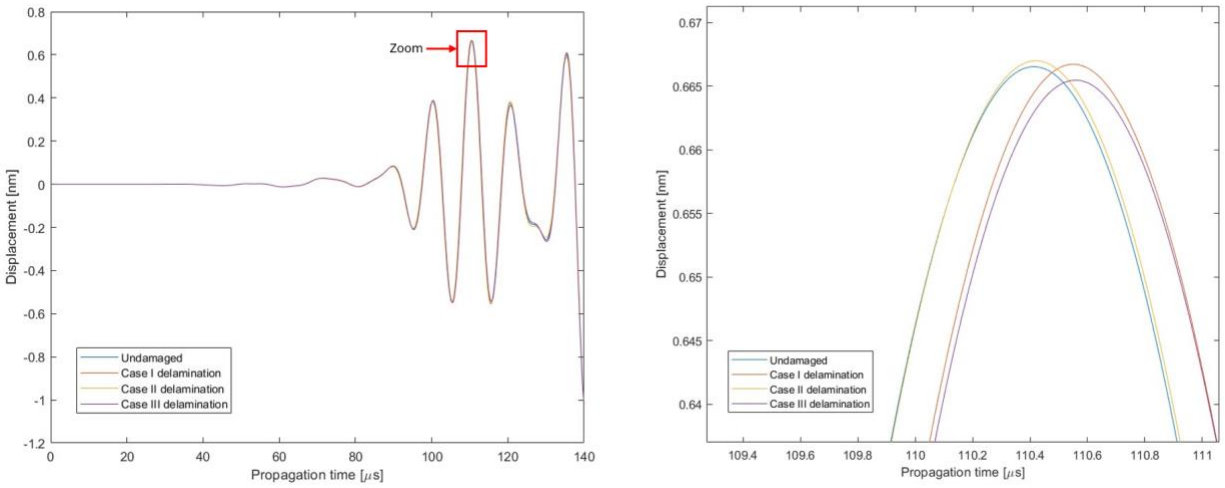

Figure 4.12: The displacement for the model containing a bolt hole for the three delamination cases and an intact plate, the right plot is a zoomed in image of the plots for comparison.

4.4 Model Variations

4.4.1 Variations in Model Thickness

Models with varying thicknesses were tested by adjusting the number of plies, and the results are presented in Figure 4.13. The model with a thickness of 2 mm, corresponding to half the original thickness, exhibited a significantly greater difference between the damaged and intact plate compared to the other thickness variations. As the crack size remains constant in all models, its impact increases as thickness decreases. The crack is positioned in the middle ply in all models. Since the excitation occurs in the top ply, a reduced number of plies brings the crack closer to the surface, leading to a greater effect on the receiver node.

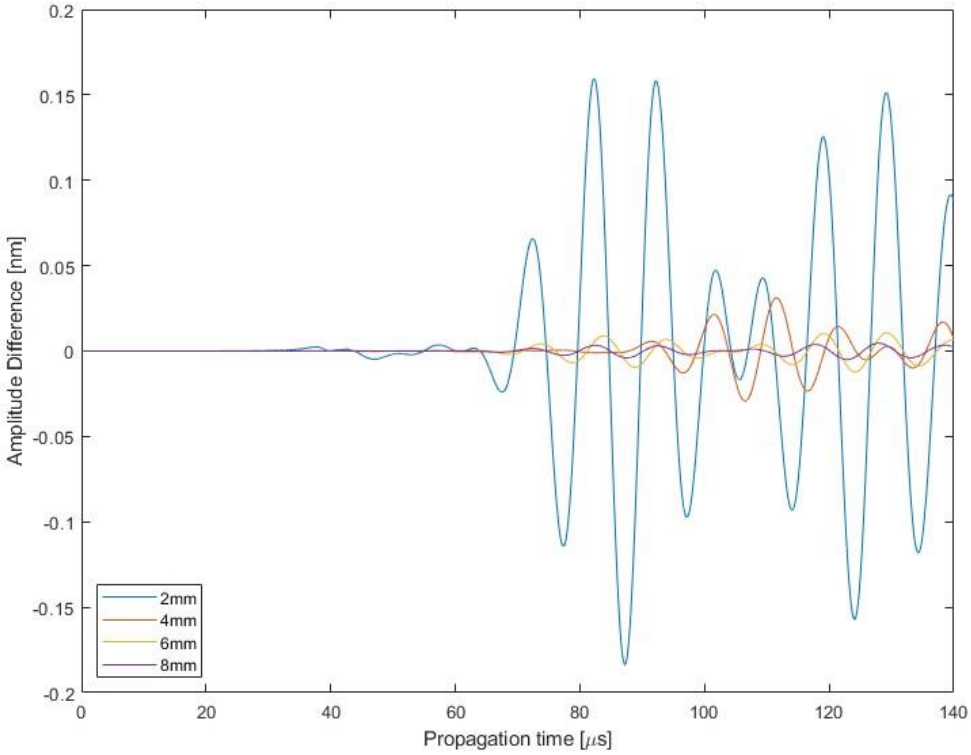

Figure 4.13: The amplitude difference for various thicknesses of the model.

4.4.2 Frequency Variations

The results from the frequency investigation are displayed in Figure 4.14, where the percentual difference in amplitude between an intact plate and a damaged plate with a 6 mm crack is plotted for the four frequencies. The results show the largest percentual difference in amplitude for 200 kHz, with a declining difference for lower frequencies. Lower frequencies typically have a deeper penetration depth compared to higher frequencies which are more sensitive to small defects. The 100 kHz frequency might thus be better suited for larger cracks, while the higher frequencies are more effective for smaller ones. This can be explained by the fact that lower frequency waves have larger wavelengths, making the difference in amplitude more pronounced if the wavelength of a lower frequency matches the crack length. If a larger defect was investigated instead,

the wavelengths of the lower frequency waves would likely be better suited for that application, as lower frequency waves should be more suitable for larger defects.

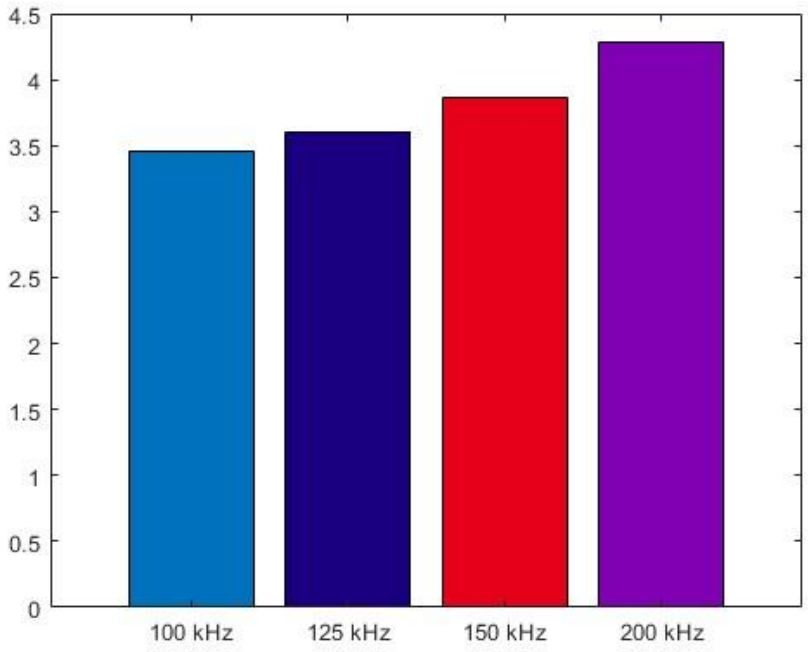

Figure 4.14: The percentual difference in amplitude between an intact and damaged plate for the four frequencies.

To investigate the impact the damage size has on the ability for different frequencies to detect damage, three more tests are performed where frequencies of 100 and 200 kHz are tested for delaminations of 6x6 mm², 2x2 mm², and 0.5x0.5 mm². Delaminations are chosen instead of cracks to investigate if the length of the damage along the wave propagation direction influences the damage detection. The results are displayed in Figure 4.15, showing that the percentual difference for 6x6 mm² is larger for 100 kHz, while 2x2 mm² and 0.5x0.5 mm² shows a larger difference for 200 kHz. This indicates that the larger wavelength of the 100 kHz frequency is more suitable for larger delaminations, since it likely matches the delamination length better, while for higher frequencies the difference for smaller delaminations and cracks is more pronounced.

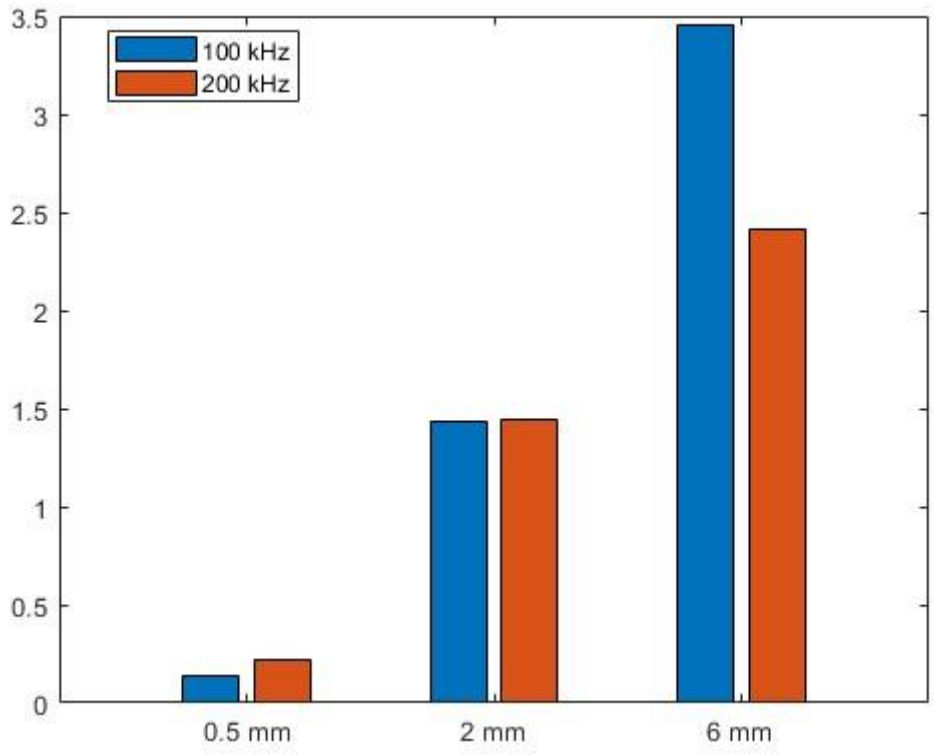

Figure 4.15: The percentual difference in amplitude between intact and damaged plates at 100 and 200 kHz frequencies for different delamination sizes.

The results from the frequency investigation indicate that different frequencies are suitable for different damage sizes. Additionally, other factors such as mesh size, simulation time, and the composite thickness play an important role in the choice of frequency. With higher frequencies comes a finer mesh size which in turn leads to longer simulation times. The frequency of 100 kHz that has been used throughout the simulations in the study is suitable for the thickness of this composite, but with thinner composites, higher frequencies might be a more appropriate choice. The choice of frequency also depends on the requirements on what damage sizes are considered a risk to the safety and health of the structure.

4.4.3 Degraded Material Properties

With the approach of modelling damages with the use of degraded material properties, the results are inconclusive. The material degradation of entire plies shows a temporal delay with an increasing number of degraded plies, displayed in Figure 4.16. A temporal delay is expected since the wave speed is dependent on the elastic properties and the density, previously mentioned in Section 2.3. Since Young's modulii and the shear modulii are degraded in all three directions of the composite while keeping the density constant, this means that the wave speed should decrease with the degradation of these properties.

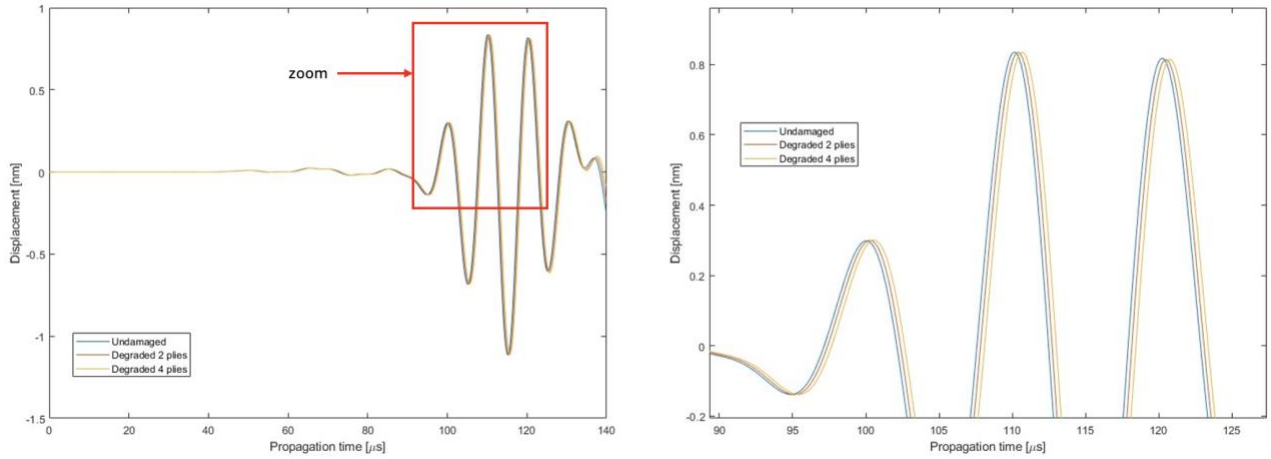

Figure 4.16: Results from the degraded material properties investigation showing a temporal delay for increasing number of degraded plies.

Meanwhile, the results from the degradation of a smaller region in the plate show a less conclusive behavior, where Figure 4.17 displays how the amplitude for the two degraded cases is increased. To replicate a modelled damage, such as a delaminated area, the amplitude should typically decrease as the wave scatters from the damage. In these cases, the amplitude increases which could be due to the transition between the non-degraded and degraded regions causing a local reflection which could change the behavior of the wave. Although the behavior of the amplitude is unconclusive, a slight temporal delay is obtained, similar to the results previously shown in Figure 4.16. This suggests that degraded material properties do in fact impact the wave speed.

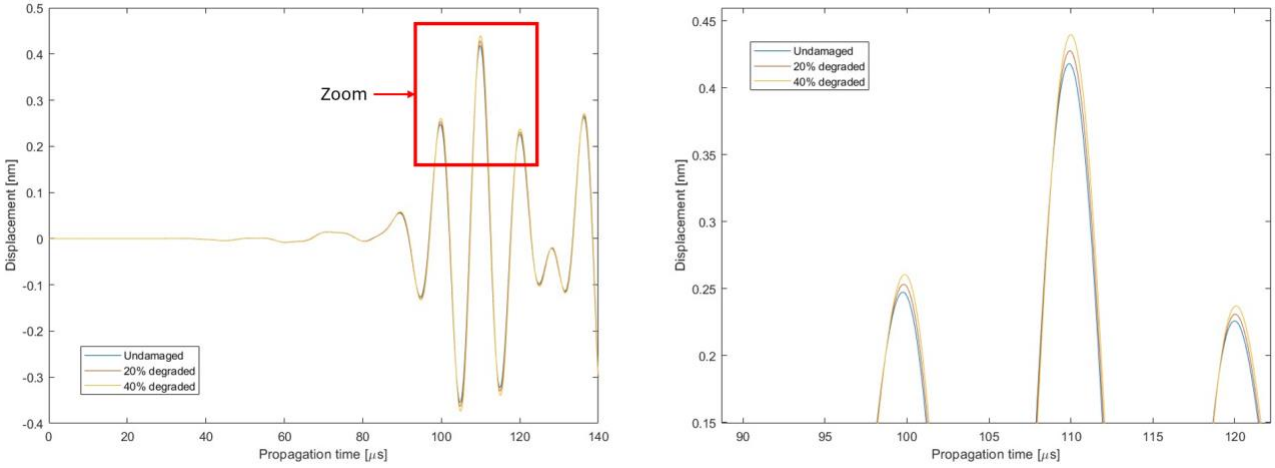

Figure 4.17: Plots of the results from the degraded region, showing an increase in amplitude with increased degradation.

To summarize the findings from the material degradation investigation, a temporal delay in wave propagation is observed when material properties are degraded. Degrading entire plies inside one layer could be useful to get an understanding of how the wave propagation changes, while keeping the simulation time manageable. However, degrading material properties in a portion of the plate to replicate damage is not considered appropriate, since the wave is likely influenced by the transition between the non-degraded and degraded regions. Moreover, accurately defining material

degradation requires experimental data and analytical models to fully understand the extent of damage-induced changes in material properties. Therefore, degradation should not be applied unless degraded properties are well characterized.

4.5 General Discussion

Various adaptations of the numerical model and the use of different frequencies have provided valuable insight into important aspects of the method's implementation. The study found that numerical damage localization is possible with the use of multiple sensors. Damage localization with the use of 8 sensors becomes less reliable when multiple damages are present. Different damage modes and sizes vary in how reliably they can be localized. Characterizing the damage would require additional simulations to develop a robust dataset or pattern that helps identify how different damage modes influence wave propagation.

Due to limitations in computing power, several simplifications were necessary, including the use of lower excitation frequencies. The frequency investigation showed that higher frequencies are more effective for detecting smaller damages. However, high frequencies are considered to be in the range of 500–1000 kHz, whilst this study only investigated frequencies up to 200 kHz. At high frequencies, the critical element size becomes smaller than the selected mesh size, as explained in Section 3.4. Refining the mesh further would result in significantly longer simulation time, as the timestep also needs to be reduced to ensure stability. Depending on the size of damage considered critical, investigating high frequencies in combination with a finer mesh should be considered if sufficient computing power is available.

These limitations also resulted in using a scaled plate model for simulations. Since one of the factors that affects the excitation signal is travel distance, using a scaled plate might lead to some misinterpretation. Testing different frequencies on a larger plate would provide further insight into which excitation signal is optimal for the application. The composite material structure was modelled as four layers instead of 32 individual layers, again due to limitations in computational power, which could have affected the results. The modelling of damages is also affected by this limitation, and a more accurate damage modelling could be evaluated with the full model.

Another limitation was the lack of experimental data to validate the numerical results with, which would be crucial when implementing the methodology at a larger scale. The results of the study could be more conclusive if there was experimental data to compare with, as this would enable fine-tuning of the boundary conditions and model parameters as well as highlighting errors in the numerical model.

Due to the lack of material data for the PZT sensors, the excitation signal was implemented through a prescribed displacement rather than electrical input. Future studies could therefore investigate the use of actual sensors with electrical input if the material data is obtained, since this could result in a more accurate representation of the propagating behavior in terms of scattering and mode conversion. This is also an important factor to consider when modelling digital twins for real-world implementations.

Future work could also investigate larger and more complex structures, as this study only focused on developing a methodology for a simple geometry. A more in-depth investigation of the geometry could provide insight into the propagating behavior of Lamb waves since curvatures, thickness discontinuities, and changes in composite layups likely could impact the results in terms of wave scattering and mode conversion. It is especially important to be able to accurately model digital twins for a real-world implementation of the method, as it is crucial to understand the propagating behavior of the structure in question.

5 Conclusion

In this study, the method of using Lamb waves for damage detection in composite structures has been evaluated and shown to be effective. Further evaluation and implementation of the SHM system could enable non-destructive testing of composite structures, contributing positively to sustainability.

By creating digital twins, numerical simulations using Lamb waves are applied to detect damage in composite structures. It is possible to simulate the electric signal that excites the Lamb waves as a prescribed displacement, which proves beneficial when PZT material data is unavailable. Additionally, the simplified composite plate model significantly helps in reducing computational cost. A difference in both time and amplitude can be used to detect variations between a damaged and intact model, with the amplitude difference being the most straightforward variation to interpret and visualize when analyzing the data.

Numerical simulations must be evaluated and refined until a reliable model is obtained. After testing various model adaptations that exhibited consistent behavior, it can be concluded that the method is reliable for damage detection. To completely evaluate the reliability of the method, experimental data must be compared with the simulations. Given that the results provide a reasonable comparison between the damaged and intact plates, while being consistent with the adaptations, the numerical method can be considered reliable.

However, to fully validate the numerical technique, experimental implementation under real-world conditions is crucial to verify the simulations. Future work should thus focus on combining the numerical approach with experimental setups, testing different composites and damage scenarios to evaluate the robustness and accuracy of the method.

6 Bibliography

[1]: Wilson, C. L.; Lonkar, K.; Roy, S.; Kopsaftopoulus, F.; Chang, F., Comprehensive Composite Materials II, Volume 7, 2018, Elsevier.
[2]: Ng, C.T.; Veidt, M., A lamb-wave-based technique for damage detection in composite laminates, Smart Materials & Structures, 2009, 18(7):1-12., IOP Publishing Ltd.
[3]: Lampeas, G.; Fotopoulus, K., Simulation of Lamb wave Propagation in Composite Structures Based on the Finite Element Stacked Shell Method, 2016, Trans Tech Publications Ltd.
[4]: Galal, M., Introduction to Composites Modelling in LS-DYNA, The Arup Campus, Blythe Gate, Blythe Valley Park, Solihull, West Midlands, UK.
[5]: Chen, B.; Zhang, Y.; Wang, Q.; Zhang, H.; Wang Y., The signal analysis of Lamb Wave in steel plates strengthened by CFRP with interface debonding, 2023, China University of Petroleum, Beijing.
[6]: Deng, P.; Saito, O.; Okabe, Y.; Soejima, H., Simplified modeling method of impact damage for numerical simulation of Lamb wave propagation in quasi-isotropic composite structures, 2020.
[7]: Kostson, E., Fatigue Crack Monitoring in Multi-Layered Aircraft Structures using Guided Ultrasonic Waves, University College London, London.
[8]: Yu, Q.; Zhou, S.; Cheng, Y.; Deng, Y., Research on Delamination Damage Quantification Detection of CFRP Bending Plate based on Lamb Wave Mode Control, 2024, Beijing Institute of Technology
[9]: Lee, B. C.; Staszewski, W. J., Modelling of Lamb waves for damage detection in metallic structures: Part I. Wave propagation, 2003, University of Sheffield, UK.
[10]: Agarwal, B. D.; Broutman, L.J.; Chandrashekara, K., Analysis and performance of fiber composites, 2006, New Jersey: John Wiley & Sons
[11]: Zenkert, D.; Battley, M., Foundations of Fibre Composites, 2:nd edition, 2020, KTH.
[12]: Clyne T. W.; Hull D., An Introduction to Composite Materials, Third Edition, 2019, Cambridge, Materials Research Society
[13]: Bhat, N.V., Delamination Growth in Graphite/Epoxy Composite Laminates Under Tensile Load, 1993, MIT
[14]: Huang, T.; Bobyr, M., A Review of Delamination Damage of Composite Materials, 2023, *J. Compos. Sci.*
[15]: Abrate S. Matrix Cracking in Laminated Composites: A review, Composites Engineering, vol. 1, 1991, University of Missouri-Rolla.
[16]: Kessler, S.S.; Spearing, S.M.; Soutis, C., Damage Detection in Composite Materials Using Lamb Wave Methods, 2002, ResearchGate
[17]: Rajput, M. Saeed, Damage Tolerance of Impacted Composite Sandwich Structures, 2018, KTH School of Engineering Sciences, Stockholm.
[18]: Wronkowicz-Katunin, A.; Katunin, A.; Dragan, K. Reconstruction of Barely Visible Impact Damage in Composite Structures Based on Non-Destructive Evaluation Results, 2019, Sensors.
[19]: Alhallak, A., PZT Scanner System For a Structural Health Monitoring Application, 2024, KTH School of Engineering Sciences, Stockholm.
[20]: Draudviliene, L.; Meskuotiene, A.; Tumsys, O.; Mazeika, L.; Samaitis, V., Metrological Performance of Hybrid Measurement Technique Applied for the Lamb Waves Phase Velocity Dispersion Evaluation, 2020, IEEE
[21]: Su, Z.; Ye, L.; LU Y., Guided Lamb waves for identification of damage in composite structures: A review, 2005, The University of Sydney, Australia

[22]: Rabbi, M.S.; Teramoto, K.; Ishibashi, H., Analytical Study on the Angular Dependency of A_0-mode Lamb Wave in Transversely Isotropic material, 2024, International Journal of Advanced Research in Basic Science
[23]: Mauritz, S., Application of Lamb waves using piezoelectric technique for structural health monitoring, 2023, KTH
[24]: Michaels, E. J.; Lee, J. S.; Croxford, J. A.; Wilcox, D., P., Chirp excitation of ultrasonic guided waves, 2012, Georgia Institute of Technology, Atlanta, USA.
[25]: P. Hora, O. Cervená, Determination of Lamb wave dispersion curves by means of Fourier transform, 2012, Institute of Thermomechanics of the ASCR, Czech Republic.
[26]: Galán-Pinilla, C. A.; E-Quiroga J.; Peña-Ballesteros D. Y.; Acosta-Minoli C. A; González-Estrada O. A, Comparative Study of Dispersion Curves for LAMB Waves Using Analytical Solutions and Semi-Analytical Methods, 2023, Universidad Industrial de Santander, Colombia.
[27]: Plesek, J.; Kolman, R., Gabriel D., Estimation of the critical time step for explicit integration, 2012, Engineering Mechanics, Svratka, Czech Republic.
[28]: Ansys Inc., Ansys LS-DYNA, Multiphysics Solver, 2025
[29]: Huber, A, The Dispersion Calculator: An Open Source Software for Calculating Dispersion Curves and Mode Shapes of Guided Waves, DLR Center for Lightweight Production Technology: Augsburg Germany, 2018
[30]: Luo, R., Saab Surveillance Gothenburg, stated April 7th 2025

7 Appendix A

The following keywords were used to define the model:

Table 7.1: Keywords used for the model.

Keyword name	Comment for use
*BOUNDARY_PRESCRIBED_MOTION_NODE	Excitation signal
*BOUNDARY_SPC_SET	Boundary conditions
*CONTACT_TIED_SURFACE_TO_SURFACE_OFFSET	Contact between layers
*CONTROL_TERMINATION	Time control
*CONTROL_TIMESTEP	Time control
*DATABASE_ASCII_option	Graphical results
*DATABASE_BINARY_D3PLOT	Graphical visualization
*DATABASE_HISTORY_NODE	Graphical results
*DEFINE_CURVE	Excitation signal/timestep
*ELEMENT_SHELL	Element formulation
*KEYWORD_KEYWORD	Model requirement
*MAT_058-LAMINATED_COMPOSITE_FABRIC	Material model
*NODE_NODE	Model nodes
*PART_PART	Used to assign composite to part
*PART_COMPOSITE	Used to assign composite to part
*SECTION_SHELL	Element formulation
*SET_NODE_LIST	Boundary conditions
*SET_SEGMENT	Damage modelling
*TITLE_TITLE	Default